APPLICATION

FOR

UNITED STATES LETTERS PATENT

BY

JORDAN J.N. TANG

LIN HONG

AND

ARUN K. GHOSH

FOR

INHIBITORS OF MEMAPSIN 2 AND USE THEREOF

INHIBITORS OF MEMAPSIN 2 AND USE THEREOF

Background of the Invention

INS A1

This application claims priority to U.S.S.N. 60/141,363 filed June 28, 1999 by Lin, et al., U.S.S.N. 60/168,060 filed November 30, 1999 by Lin, et al., U.S.S.N. 60/177,836 filed January 25, 2000 by Lin, et al., U.S.S.N. 60/178,368 filed January 27, 2000 by Lin, et a., and U.S.S.N. 60/210,292 filed June 8, 2000 by Lin Hong, et al., the teachings of which are incorporated by reference herein.

This invention is in the area of the design and synthesis of specific inhibitors of the aspartic protease Memapsin 2 (beta-secretase) which are useful in the treatment and/or prevention of Alzheimer's Disease.

Alzheimer's disease (AD) is a degenerative disorder of the brain first described by Alios Alzheimer in 1907 after examining one of his patients who suffered drastic reduction in cognitive abilities and had generalized dementia (*The early story of Alzheimer's Disease*, edited by Bick *et al.* (Raven Press, New York 1987)). It is the leading cause of dementia in elderly persons. AD patients have increased problems with memory loss and intellectual functions which progress to the point where they cannot function as normal individuals. With the loss of intellectual skills the patients exhibit personality changes, socially inappropriate actions and schizophrenia (*A Guide to the Understanding of Alzheimer's Disease and Related Disorders*, edited by Jorm (New York University Press, New York 1987). AD is devastating for both victims and their families, for there is no effective palliative or preventive treatment for the inevitable neurodegeneration.

AD is associated with neuritic plaques measuring up to 200 μm in diameter in the cortex, hippocampus, subiculum, hippocampal gyrus, and amygdala. One of the principal constituents of neuritic plaques is amyloid, which is stained by Congo Red (Fisher (1983); Kelly Microbiol. Sci. 1(9):214-219 (1984)). Amyloid plaques stained by Congo Red are extracellular, pink or rust-colored in bright field, and birefringent in polarized light. The plaques are composed of polypeptide fibrils and are often present around blood vessels, reducing blood supply to various neurons in the brain.

Various factors such as genetic predisposition, infectious agents, toxins, metals, and head trauma have all been suggested as possible mechanisms of AD neuropathy. Available evidence strongly indicates that there are distinct types of genetic predispositions for AD. First, molecular analysis has provided evidence for mutations in the amyloid precursor protein (APP) gene in certain AD-stricken families (Goate *et al. Nature* 349:704-706 (1991); Murrell *et al. Science* 254:97-99 (1991); Chartier-Harlin *et al. Nature* 353:844-846 (1991); Mullan *et al., Nature Genet.* 1:345-347 (1992)). Additional genes for dominant forms of early onset AD reside on chromosome 14 and chromosome 1 (Rogaev *et al., Nature* 376:775-778 (1995); Levy-Lahad *et al., Science* 269:973-977 (1995); Sherrington *et al., Nature* 375:754-760 (1995)). Another loci associated with AD resides on chromosome 19 and encodes a variant form of apolipoprotein E (Corder, *Science* 261:921-923 (1993)).

Amyloid plaques are abundantly present in AD patients and in Down's Syndrome individuals surviving to the age of 40. The overexpression of APP in Down's Syndrome is recognized as a possible cause of the development of AD in Down's patients over thirty years of age (Rumble *et al., New England J. Med.* 320:1446-1452 (1989); Mann *et al., Neurobiol. Aging* 10:397-399 (1989)). The plaques are also present in the normal aging brain, although at a lower number. These plaques are made up primarily of the amyloid β peptide (Aβ; sometimes also referred to in the literature as β-amyloid peptide or β peptide) (Glenner and Wong, *Biochem. Biophys. Res. Comm.* 120:885-890 (1984)), which is also the primary protein constituent in cerebrovascular amyloid deposits. The amyloid is a filamentous material that is arranged in beta-pleated sheets. Aβ is a hydrophobic peptide comprising up to 43 amino acids.

The determination of its amino acid sequence led to the cloning of the APP cDNA (Kang *et al., Nature* 325:733-735 (1987); Goldgaber *et al., Science* 235:877-880 (1987); Robakis *et al., Proc. Natl. Acad. Sci.* 84:4190-4194 (1987); Tanzi *et al., Nature* 331:528-530 (1988)) and genomic APP DNA (Lemaire *et al., Nucl. Acids Res.* 17:517-522 (1989); Yoshikai *et al., Gene* 87, 257-263 (1990)). A number of forms of APP cDNA have been identified, including the

three most abundant forms, APP695, APP751, and APP770. These forms arise from a single precursor RNA by alternate splicing. The gene spans more than 175 kb with 18 exons (Yoshikai *et al.* (1990)). APP contains an extracellular domain, a transmembrane region and a cytoplasmic domain. Aβ consists of up to 28 amino acids just outside the hydrophobic transmembrane domain and up to 15 residues of this transmembrane domain. Aβ is normally found in brain and other tissues such as heart, kidney and spleen. However, Aβ deposits are usually found in abundance only in the brain.

Van Broeckhaven *et al.*, *Science* 248:1120-1122 (1990), have demonstrated that the APP gene is tightly linked to hereditary cerebral hemorrhage with amyloidosis (HCHWA-D) in two Dutch families. This was confirmed by the finding of a point mutation in the APP coding region in two Dutch patients (Levy *et al.*, *Science* 248:1124-1128 (1990)). The mutation substituted a glutamine for glutamic acid at position 22 of the Aβ (position 618 of APP695, or position 693 of APP770). In addition, certain families are genetically predisposed to Alzheimer's disease, a condition referred to as familial Alzheimer's disease (FAD), through mutations resulting in an amino acid replacement at position 717 of the full length protein (Goate *et al.* (1991); Murrell *et al.* (1991); Chartier-Harlin *et al.* (1991)). These mutations co-segregate with the disease within the families and are absent in families with late-onset AD. This mutation at amino acid 717 increases the production of the $A\beta_{1-42}$ form of Aβ from APP (Suzuki *et al.*, *Science* 264:1336-1340 (1994)). Another mutant form contains a change in amino acids at positions 670 and 671 of the full length protein (Mullan *et al.* (1992)). This mutation to amino acids 670 and 671 increases the production of total Aβ from APP (Citron *et al.*, *Nature* 360:622-674 (1992)).

APP is processed *in vivo* at three sites. The evidence suggests that cleavage at the ß -secretase site by a membrane associated metalloprotease is a physiological event. This site is located in APP 12 residues away from the lumenal surface of the plasma membrane. Cleavage of the ß -secretase site (28 residues from the plasma membrane's lumenal surface) and the ß -secretase site

(in the transmembrane region) results in the 40/42-residue ß -amyloid peptide (A ß), whose elevated production and accumulation in the brain are the central events in the pathogenesis of Alzheimer's disease (for review, see Selkoe, D.J. *Nature* 399:23-31 (1999)). Presenilin 1, another membrane protein found in human brain, controls the hydrolysis at the APP (ß -secretase site and has been postulated to be itself the responsible protease (Wolfe, M.S.et al., *Nature* 398:513-517 (1999)). Presenilin 1 is expressed as a single chain molecule and its processing by a protease, presenilinase, is required to prevent it from rapid degradation (Thinakaran, G. et al., *Neuron* 17:181-190 (1996) and Podlisny, M.B., et al., *Neurobiol. Dis.* 3:325-37 (1997)). The identity of presenilinase is unknown. The *in vivo* processing of the ß -secretase site is thought to be the rate-limiting step in A ß production (Sinha, S. & Lieberburg, I., *Proc. Natl. Acad. Sci., USA,* 96:11049-11053 (1999)), and is therefore a strong therapeutic target.

The design of inhibitors effective in decreasing amyeloid plaque formation is dependent on the identification of the critical enzyme(s) in the cleavage of APP to yield the 42 amino acid peptide, the $A\beta_{1-42}$ form of $A\beta$. Although several enzymes have been identified, it has not been possible to produce active enzyme. Without active enzyme, one cannot confirm the substrate specificity, determine the subsite specificity, nor determine the kinetics or critical active site residues, all of which are essential for the design of inhibitors.

Memapsin 2 has been shown to be beta-secretase, a key protease involved in the production in human brain of beta-amyloid peptide from beta-amyloid precursor protein (for review, see Selkoe, D.J. *Nature* 399:23-31 (1999)). It is now generally accepted that the accumulation of beta- amyloid peptide in human brain is a major cause for the Alzheimer's disease. Inhibitors specifically designed for human memapsin 2 should inhibit or decrease the formation of beta-amyloid peptide and the progression of the Alzheimer's disease.

Memapsin 2 belongs to the aspartic protease family. It is homologous in amino acid sequence to other eukaryotic aspartic proteases and contains motifs specific to that family. These structural similarities predict that memapsin 2 and other eukaryotic aspartic proteases share common catalytic mechanism Davies, D.R., *Annu. Rev. Biophys. Chem.* 19, 189 (1990). The most successful inhibitors for aspartic proteases are mimics of the transition state of these enzymes. These inhibitors have substrate-like structure with the cleaved planar peptide bond between the carbonyl carbon and the amide nitrogen replaced by two tetrahedral atoms, such as hydroxyethylene [-CH(OH)-CH_2-], which was originally discovered in the structure of pepstatin (Marciniszyn et al., 1976).

However, for clinical use, it is preferable to have small molecule inhibitors which will pass through the blood brain barrier and which can be readily synthesized. It is also desirable that the inhibitors are relatively inexpensive to manufacture and that they can be administered orally. Screening of thousands of compounds for these properties would require an enormous effort. To rationally design memapsin 2 inhibitors for treating Alzheimer's disease, it will be important to know the three-dimensional structure of memapsin 2, especially the binding mode of an inhibitor in the active site of this protease.

It is therefore an object of the present invention to provide purified, recombinant, and active memapsin 2, as well as its substrate and subsite specificity and critical active site residues.

It is a further object of the present invention to provide compositions and methods for synthesis of inhibitors of memapsin 2.

It is a still further object of the present invention to provide compositions that interact with memapsin 2 or its substrate to inhibit cleavage by the memapsin 2 which can cross the blood brain barrier (BBB).

It is therefore an object of the present invention to provide means for rational design and screening of compounds for inhibition of mamapsin 2.

Summary of the Invention

Methods for the production of purified, catalytically active, recombinant memapsin 2 have been developed. The substrate and subsite specificity of the catalytically active enzyme have been determined. The active enzyme and assays for catalytic activity are useful in screening libraries for inhibitors of the enzyme.

The substrate and subsite specificity information was used to design substrate analogs of the natural memapsin 2 substrate that can inhibit the function of memapsin 2. The substrate analogs are based on peptide sequences, shown to be related to the natural peptide substrates for memapsin 2. The substrate analogs contain at least one analog of an amide (peptide) bond which is not capable of being cleaved by memapsin 2. Processes for the synthesis of two substrate analogues including isosteres at the sites of the critical amino acid residues were developed and the substrate analogues, OMR99-1 and OM99-2, were synthesized. OM99-2 is based on an octapeptide Glu-Val-Asn-Leu-Ala-Ala-Glu-Phe (SEQ ID NO:28) with the Leu-Ala peptide bond substituted by a transition-state isostere hydroxyethylene group. The inhibition constant of OM99-2 is1.6 x 10^{-9} M against recombinant pro-memapsin 2. Crystallography of memapsin 2 bound to this inhibitor was used to determine the three dimensional structure of the protein, as well as the importance of the various residues in binding.

This information can be used by those skilled in the art to design new inhibitors, using commercially available software programs and techniques familiar to those in organic chemistry and enzymology, to design new inhibitors. For example, the side chains of the inhibitors may be modified to produce stronger interactions (through hydrogen bonding, hydrophobic interaction, charge interaction and/or van der Waal interaction) in order to increase inhibition potency. Based on this type of information, the residues with minor interactions may be eliminated from the new inhibitor design to decrease the molecular weight of the inhibitor. The side chains with no structural hindrance from the enzyme may be cross-linked to lock in the effective

inhibitor conformation. This type of structure also enables the design of peptide surrogates which may effectively fill the binding sites of memapsin 2 yet produce better pharmaceutical properties.

The examples demonstrate the production of catalytically active enzyme, design and synthesis of inhibitors, and how the crystal structure was obtained. The examples thereby demonstrate how the methods and materials described herein can be used to screen libraries of compounds for other inhibitors, as well as for design of inhibitors. These inhibitors are useful in the prevention and/or treatment of Alzheimer's disease as mediated by the action of the beta secretase memapsin 2, in cleaving APP.

Brief Description of the Drawings

Figure 1 depicts the plasmid construct of vector pET-11a-memapsin 2-T1 and pET-11a-memapsin 2-T2. The T7 promotor, amino acid sequence from the vector (T7 protein) (SEQ ID NO:3), and the beginning and ending of the memapsin 2 T1 and T2 construct are shown. Construct promemapsin 2-T1 was used in the preparation of protein for crystallization and includes residues 1v-15v which are derived from vector pET-11a. Residues 1p-48p are putative pro-peptide. Residues 1-393 correspond to the mature protease domain and C-terminal extension. The residue numbering of memapsin 2 starts at the aligned N-terminal position of pepsin ~~(Figure 3).~~ Figures 3A and 3B

Figure 2A is a graph of the initial rate of hydrolysis of synthetic peptide swAPP (see Table 1) by $M2_{pd}$ at different pH. Figure 2B is a graph of the relative k_{cat}/K_m values for steady-state kinetic of hydrolysis of peptide substrates by $M2_{pd}$.

Figures 3A and 3B are the chemical structures of memapsin 2 inhibitors, ~~OM99-2 and OM99-1.~~ OM99-1 AND OM99-2

Figure 4A is a graph of the inhibition of recombinant memapsin 2 by OM99-1. Figure 4B is a graph of the inhibition of recombinant memapsin 2 by OM99-2.

Figures 5A-E are photographs of crystals of recombinant memapsin 2-OM99-2 complex.

Figure 6 is a stereo view of crystal structure of memapsin 2 protease domain with bound OM99-2.The polypeptide backbone of memapsin 2 is shown as a ribbon diagram. The N-lobe and C- lobe are blue and yellow, respectively, except the insertion loops (designated A to G, see ~~Figure 2)~~ FIGURE 6 in the C-lobe are magenta and the C-terminal extension is green. The inhibitor bound between the lobes is shown in red.

Figure 7 is a stereo view of comparison of the three-dimensional structures of memapsin 2 and pepsin. The molecular surface of the former is significantly larger by the insertion of surface loops and helix and the C-terminal extension. Chain tracing of human memapsin 2 is dark blue and is grey for human pepsin. The light blue balls represent identical residues which are topologically equivalent. The disulfide bonds are shown in red for memapsin 2 and orange for pepsin. The C-terminal extension is in green.

Figure 8 is a schematic presentation of interaction between OM99-2 and memapsin 2 protease domain. The S_3' and S_4' subsites are not defined.

Figure 9 is a stereo presentation of interactions between inhibitor OM99-2 (orange) and memapsin 2 (light blue). Nitrogen and oxygen atoms are marked blue and red, respectively. Hydrogen bonds are indicated in yellow dotted lines. Memapsin 2 residues which comprise the binding subsites are included. Residues P_4, P_3, P_2, P_1 and P_1' (defined in Figure 8) of OM99-2 are in an extended conformation. Inhibitor chain turns at residue P2' which makes a distinct kink at this position. The backbone of P_3' and P_4' directs the inhibitor to exit the active site.

Figure 10 are schematics of the cross linking between P_3 Val and P_1 Leu side chains in the design of new inhibitors for memapsin 2 based on the current crystal structure. R and R' at positions P_2 and P_1' indicate amino acid side chains. Other structural elements of inhibitor are omitted for clarity.

Figure 11 are schematics of the cross linking between P_4 Glu and P_2 Asn side chains in the design of new inhibitors for memapsin 2 based on the current crystal structure. R at position P_3 indicates amino acid side chain. Other structural elements of inhibitor are omitted for clarity.

Figure 12 is a schematic of the design for the side chain at the P_1' subsite for the new memapsin 2 inhibitors based on the current crystal structure. Arrows indicate possible interactions between memapsin 2 and inhibitor. Other structural elements of inhibitor are omitted for clarity.

Figure 13 is a schematic of the design of two six-membered rings in the inhibitor structure by the addition of atoms A and B. The ring formation involves the P_1-Leu side chain the the peptide backbone near P_1, P_2, and P_3. The new bonds are in dotted lines. A methyl group can be added to the beta-carbon of P_1-Leu. Other structural elements of inhibitor are omitted for clarity.

Detailed Description of the Invention

I. <u>Preparation of Catalytically Active Recombinant Memapsin 2</u>

<u>Cloning and Expression of Memapsin 2</u>

Memapsin 2 was cloned and the nucleotide (SEQ ID NO. 1) and predicted amino acid (SEQ ID NO. 2) sequences were determined, as described in Example 1. The cDNA was assembled from the fragments. The nucleotide and the deduced protein sequence are shown in SEQ ID NOs. 1 and 2, respectively. The protein is the same as the aspartic proteinase 2 (ASP2) described in EP 0 855 444 A by SmithKline Beecham Pharmaceuticals, (published July 29, 1998), and later reported by Sinha, et al., Nature 402, 537-540 (December 1999) and Vassar, et al., Science 286, 735-741 (22 October 1999).

Pro-memapsin 2 is homologous to other human aspartic proteases. Based on the alignments, Pro-memapsin 2 contains a *pro* region, an aspartic protease region, and a trans-membrane region near the C-terminus. The C-terminal domain is over 80 residues long. The active enzyme is memapsin 2 and its pro-enzyme is pro-memapsin 2.

<u>Refolding Catalytically Active Enzyme</u>

In order to determine the substrate specificity and to design inhibitors, it is necessary to express catalytically active recombinant enzyme. No other known proteases contain a transmembrane domain. The presence of transmembrane domains makes the recombinant expression of these proteins

less predictable and more difficult. The transmembrane region often needs to be removed so that secretion of the protein can take place. However, the removal of the transmembrane region can often alter the structure and/or function of the protein.

The starting assumption was that the region of memapsin 2 that is homologous with other aspartic proteases would independently fold in the absence of the transmembrane domain, and would retain protease activity in the absence of the C-terminal transmembrane region. The transmembrane region appears to serve as a membrane anchor. Since the active site is not in the transmembrane region and activity does not require membrane anchoring, memapsin 2 was expressed in *E. coli* in two different lengths, both without the transmembrane region, and purified, as described in Example 3. The procedures for the culture of transfected bacteria, induction of synthesis of recombinant proteins and the recovery and washing of inclusion bodies containing recombinant proteins are essentially as described by Lin et al., (1994). Refolding was not a simple matter, however. Two different refolding methods both produced satisfactory results. In both methods, the protein was dissolved in a strong denaturing/reducing solution such as 8 M urea/100 mM beta-mercaptoethanol. The rate at which the protein was refolded, and in what solution, was critical to activity. In one method, the protein is dissolved into 8 M urea/100 mM beta-mercaptoethanol then rapidly diluted into 20 volumes of 20 mM-Tris, pH 9.0, which is then slowly adjusted to pH 8 with 1 M HCl. The refolding solution was then kept at 4° C for 24 to 48 hours before proceeding with purification. In the second method, an equal volume of 20 mM Tris, 0.5 mM oxidized/1.25 mM reduced glutathione, pH 9.0 is added to rapidly stirred pro-memapsin 2 in 8 M urea/10 mM beta-mercaptoethanol. The process is repeated three more times with 1 hour intervals. The resulting solution is then dialyzed against sufficient volume of 20 mM Tris base so that the final urea concentration is 0.4 M. The pH of the solution is then slowly adjusted to 8.0 with 1 M HCl.

The refolded protein is then further purified by column chromatography, based on molecular weight exclusion, and/or elution using a salt gradient, and analyzed by SDS-PAGE analysis under reduced and non-reduced conditions.

II. Substrate Specificity and Enzyme Kinetics of Memapsin 2

Substrate Specificity

The tissue distribution of the memapsin 2 was determined, as described in Example 2. The presence of memapsin 2 (M2) in the brain indicated that it might hydrolyze the β-amyloid precursor protein (APP). As described below, detailed enzymatic and cellular studies demonstrated that M2 fits all the criteria of the ß-secretase.

The M2 three-dimensional structure modeled as a type I integral membrane protein. The model suggested that its globular protease unit can hydrolyze a membrane anchored polypeptide at a distance range of 20-30 residues from the membrane surface. As a transmembrane protein of the brain, APP is a potential substrate and its beta-secretase site, located about 28 residues from the plasma membrane surface, is within in the range for M2 proteolysis.

A synthetic peptide derived from this site (SEVKM/DAEFR) (SEQ ID NO:4) was hydrolyzed by $M2_{pd}$ (modified M2 containing amino acids from Ala^{-8P} to Ala^{326}) at the beta-secretase site (marked by /). A second peptide (SEVNL/DAEFR) (SEQ ID NO:5) derived from the APP beta-secretase site and containing the 'Swedish mutation' (Mullan, M. *et al., Nature Genet.* 2:340-342 (1992)), known to elevate the level of alpha-beta production in cells (Citron, M. et al., *Nature* 260:672-674 (1992)), was hydrolyzed by $M2_{pd}$ with much higher catalytic efficiency. Both substrates were optimally cleaved at pH 4.0. A peptide derived from the processing site of presenilin 1 (SVNM/AEGD) (SEQ ID NO:6) was also cleaved by $M2_{pd}$ with less efficient kinetic parameters. A peptide derived from the APP gamma-secretase site (KGGVVIATVIVK) (SEQ ID NO:7) was not cleaved by $M2_{pd}$. Pepstatin A inhibited $M2_{pd}$ poorly (IC_{50} approximately approximately 0.3 mM). The kinetic parameters indicate that both presenilin 1 (k_{cat}, 0.67 s^{-1}; K_m, 15.2 mM; k_{cat}/K_m, 43.8 $s^{-1}M^{-1}$) and native

APP peptides (k_{cat}/K_m, 39.9 $s^{-1}M^{-1}$) are not as good substrates as the Swedish APP peptide (k_{cat}, 2.45 s^{-1},K_m, 1 mM; k_{cat}/K_m, 2450 $s^{-1}M^{-1}$).

To determine if M2 possesses an APP beta-secretase function in mammalian cells, memapsin 2 was transiently expressed in HeLa cells (Lin, X., et al., *FASEB J.* 7:1070-1080 (1993)), metabolically pulse-labeled with ^{35}S-Met, then immunoprecipitated with anti-APP antibodies for visualization of APP-generated fragments after SDS-polyacrylamide electrophoresis and imaging. SDS-PAGE patterns of immuno-precipitated APP Nß-fragment (97 kD band) from the conditioned media (2 h) of pulse-chase experiments showed that APP was cleaved by M2. Controls transfected with APP alone and co-transfected with APP and M2 with Bafilomycin A1 added were performed. SDS-PAGE patterns of APP ßC-fragment (12 kD) were immunoprecipitated from the conditioned media of the same experiment as discussed above. Controls transfected with APP alone; co-transfected with APP and M2; co-transfected with APP and M2 with Bafilomycin A1; transfections of Swedish APP; and co-transfections of Swedish APP and M2 were performed. SDS-PAGE gels were also run of immuno-precipitated M2 (70 kD), M2 transfected cells; untransfected HeLa cells after long time film exposure; and endogenous M2 from HEK 293 cells. SDS-PAGE patterns of APP fragments (100 kD betaN-fragment and 95 kD betaN-fragment) recovered from conditioned media after immuno-precipitation using antibodies specific for different APP regions indicated that memapsin 2 cleaved APP.

Cells expressing both APP and M2 produced the 97 kD APP beta N-fragment (from the N-terminus to the beta-secretase site) in the conditioned media and the 12 kD betaC-fragment (from the beta-secretase site to the C-terminus) in the cell lystate. Controls transfected with APP alone produced little detectable betaN-fragment and no beta C-fragment. Bafilomycin A1, which is known to raise the intra-vesicle pH of lysosomes/endosomes and has been shown to inhibit APP cleavage by beta-secretase (Knops, J. et al., *J. Biol. Chem.* 270:2419-2422 (1995)), abolished the production of both APP fragments beta N- and beta C- in co-transfected cells. Cells transfected with Swedish APP

alone did not produce the beta C-fragment band in the cell lysate but the co-transfection of Swedish APP and M2 did. This Swedish beta C-fragment band is more intense than that of wild-type APP. A 97-kD beta N-band is also seen in the conditioned media but is about equal intensity as the wild-type APP transfection.

These results indicate that M2 processes the beta-secretase site of APP in acidic compartments such as the endosomes. To establish the expression of transfected M2 gene, the pulse-labeled cells were lysed and immuno-precipitated by anti-M2 antibodies. A 70 kD M2 band was seen in cells transfected with M2 gene, which has the same mobility as the major band from HEK 293 cells known to express beta-secretase (Citron, M. et al., *Nature* 260:672-674 (1992)). A very faint band of M2 is also seen, after a long film exposure, in untransfected HeLa cells, indicating a very low level of endogenous M2, which is insufficient to produce betaN- or betaC-fragments without M2 transfection. Antibody alpha-beta$_{1-17}$, which specifically recognizes residues 1-17 in alpha-beta peptide, was used to confirm the correct beta-secretase site cleavage. In cells transfected with APP and M2, both beta N- and beta N-fragments are visible using an antibody recognizing the N-terminal region of APP present in both fragments. Antibody Abeta$_{1-17}$ recognize the beta N-fragment produced by endogenous beta-secretase in the untransfected cells. This antibody was, however, unable to recognize the betaN-fragment known to be present in cells co-transfected with APP and M2. These observations confirmed that betaN-fragment is the product of beta-secretase site cut by M2, which abolished the recognition epitope of alpha-beta$_{1-17}$.

The processing of APP by M2 predicts the intracellular colocalization of the two proteins. HeLa cells co-expressing APP and M2 were stained with antibodies directed toward APP and M2 and visualized simultaneously by CSLM using a 100x objective. Areas of colocalization appeared in yellow.

Immunodetection observed by confocal microscopy of both APP and M2 revealed their colocalization in the superimposed scans. The distribution of both

proteins is consistent with their residence in lysosomal/endosomal compartments.

In specificity studies, it was found that $M2_{pd}$ cleaved its *pro* peptide (2 sites) and the protease portion (2 sites) during a 16 h incubation after activation (Table 1). Besides the three peptides discussed above, $M2_{pd}$ also cleaved oxidized bovine insulin B chain and a synthetic peptide Nch. Native proteins were not cleaved by $M2_{pd}$.

The data indicate that human M2 fulfills all the criteria of a beta-secretase which cleaves the beta-amyloid precursor protein (APP): (a) M2 and APP are both membrane proteins present in human brain and co-localize in mammalian cells, (b) M2 specifically cleaves the beta-secretase site of synthetic peptides and of APP in cells, (c) M2 preferentially cleaves the beta-secretase site from the Swedish over the wild-type APP, and (d) the acidic pH optimum for M2 activity and bafilomycin A1 inhibition of APP processing by M2 in the cells are consistent with the previous observations that beta-secretase cleavage occurs in acidic vesicles (Knops, J., et al., *J. Biol. Chem.* 270:2419-2422 (1995)). The spontaneous appearance of activity of recombinant pro-M2 in an acidic solution suggests that, intracellularly, this zymogen can by itself generate activity in an acidic vesicle like an endosome.

II. <u>Design and Synthesis of Inhibitors</u>

<u>Design of Substrate Analogs for Memapsin 2.</u>

The five human aspartic proteases have homologous amino acid sequences and have similar three-dimensional structures. There are two aspartic residues in the active site and each residue is found within the signature aspartic protease sequence motif, Asp-Thr/Ser-Gly- (SEQ ID NO:8). There are generally two homologous domains within an aspartic protease and the substrate binding site is positioned between these two domains, based on the three-dimensional structures. The substrate binding sites of aspartic proteases generally recognize eight amino acid residues. There are generally four residues on each side of the amide bond which is cleaved by the aspartic protease.

Typically the side chains of each amino acid are involved in the specificity of the substrate/aspartic protease interaction. The side chain of each substrate residue is recognized by regions of the enzyme which are collectively called sub-sites. The generally accepted nomenclature for the protease sub-sites and their corresponding substrate residues are shown below, where the double slash represents the position of bond cleavage.

Protease sub-sites	S4	S3	S2	S1	S1'	S2'	S3'	S4'
Substrate residues	P4	P3	P2	P1 //	P1'	P2'	P3'	P4'

While there is a general motif for aspartic protease substrate recognition, each protease has a very different substrate specificity and breadth of specificity. Once the specificity of an aspartic protease is known, inhibitors can be designed based on that specificity, which interact with the aspartic protease in a way that prevents natural substrate from being efficiently cleaved. Some aspartic proteases have specificities which can accommodate many different residues in each of the sub-sites for successful hydrolysis. Pepsin and cathepsin D have this type of specificity and are said to have "broad" substrate specificity. When only a very few residues can be recognized at a sub-site, such as in renin, the aspartic protease is said to have a stringent or narrow specificity.

The information on the specificity of an aspartic protease can be used to design specific inhibitors in which the preferred residues are placed at specific sub-sites and the cleaved peptide bond is replaced by an analog of the transition-state. These analogs are called transition state isosteres. Aspartic proteases cleave amide bonds by a hydrolytic mechanism. This reaction mechanism involves the attack by a hydroxide ion on the ß-carbon of the amino acid. Protonation must occur at the other atom attached to the ß-carbon through the bond that is to be cleaved. If the ß-carbon is insufficiently electrophilic or the atom attached to the bond to be cleaved is insufficiently nucleophilic the bond will not be cleaved by a hydrolytic mechanism. Analogs exist which do not mimic the transition state but which are non-hydrolyzable, but transition state isosteres mimic the transition state specifically and are non-hydrolyzable.

Transition state theory indicates that it is the transition state intermediate of the reaction which the enzyme catalyzes for which the enzyme has its highest affinity. It is the transition state structure, not the ground state structure, of the substrate which will have the highest affinity for its given enzyme. The transition state for the hydrolysis of an amide bond is tetrahedral while the ground state structure is planar. A typical transition-state isostere of aspartic protease is -CH(OH)-CH_2-, as was first discovered in pepstatin by Marciniszyn et al. (1976). The transition-state analogue principles have been successfully applied to inhibitor drugs for human immunodeficiency virus protease, an aspartic protease. Many of these are currently in clinical use. Information on the structure, specificity, and types of inhibitors can be found in Tang, Acid Proteases, Structure, Function and Biology, Adv. in Exptl. Med. Biol. vol. 95 (Plenum Press, NY 1977); Kostka, Aspartic Proteinases and their Inhibitors (Walter de Gruyter, Berlin 1985); Dunn, Structure and Functions of the Aspartic Proteinases, Adv. in Exptl. Med. Biol. 306 (Plenum Press, NY 1991); Takahashi, Aspartic Proteases, Structure, Function, Biology, Biomedical Implications, Adv. in Exptl. Med. Biol. 362 (Plenum Press, NY 1995); and James, Aspartic Proteinases, Retroviral and Cellular Enzymes, Adv. in Exptl. Med. Biol. 436 (Plenum Press, NY 1998)).

Substrate analog compositions are generally of the general formula X-L_4-P_4- L_3-P_3-L_2-P_2-L_1-P_1-L_0-P_1'-L_1'-P_2'-L_2'-P_3'-L_3'-P_4'L_4'-Y. The substrate analog compositions are analogs of small peptide molecules. Their basic structure is derived from peptide sequences that were determined through structure/function studies. It is understood that positions represented by P_x represent the substrate specificity position relative to the cleavage site which is represented by an –L_0-. The positions of the compositions represented by L_x represent the linking regions between each substrate specificity position, P_x.

In a natural substrate for memapsin 2, a P_x-L_x pair would represent a single amino acid of the peptide which is to be cleaved. In the present general formula, each P_x part of the formula refers to the α-carbon and side chain functional group of each would be amino acid. Thus, the P_x portion of an P_x-L_x

pair for alanine represents HC- CH_3. The general formula representing the P_x portion of the general composition is $-R_1CR_3-$.

In general R_1 can be either CH_3 (side chain of alanine), $CH(CH_3)_2$ (side chain of valine), $CH_2CH(CH_3)_2$ (side chain of leucine), $(CH_3)CH(CH_2\ CH_3)$ (side chain of isoleucine), CH_2(Indole) (side chain of tryptophan), CH_2(Benzene) (side chain of phenylalanine), $CH_2CH_2SCH_3$ (side chain of methionine), H (side chain of glycine), CH_2OH (side chain of serine), $CHOHCH_3$ (side chain of threonine), CH_2(Phenol) (side chain of tyrosine), CH_2SH (side chain of cysteine), $CH_2CH_2CONH_2$ (side chain of glutamine), CH_2CONH_2 (side chain of asparagine), $CH_2CH_2CH_2CH_2NH_2$ (side chain of lysine), $CH_2CH_2CH_2NHC(NH)(NH_2)$ (side chain of arginine), CH_2(Imidazole) (side chain of histidine), CH_2COOH (side chain of aspartic acid), CH_2CH_2COOH (side chain of glutamic acid), and functional natural and non-natural derivatives or synthetic substitutions of these.

It is most preferred that R_3 is a single H. In general, however, R_3 can be alkenyl, alkynal, alkenyloxy, and alkynyloxy groups that allow binding to memapsin 2. Preferably, alkenyl, alkynyl, alkenyloxy and alkynyloxy groups have from 2 to 40 carbons, and more preferably from 2 to 20 carbons, from 2 to 10 carbons, or from 2 to 3 carbons., and functional natural and non-natural derivatives or synthetic substitutions of these.

The L_x portion of the P_x-L_x pair represents the atoms linking the P_x regions together. In a natural substrate the L_x represents the ß-carbon attached to the amino portion of what would be the next amino acid in the chain. Thus, L_x would be represented by –CO-NH-. The general formula for L_x is represented by R_2. In general R_2 can be CO-HN (amide), $CH(OH)(CH_2)$ (hydroxyethylene), $CH(OH)CH(OH)$ (dihydroxyethylene), $CH(OH)CH_2NH$ (hydroxyethylamine), $PO(OH)CH_2$ (phosphinate), CH_2NH, (reduced amide). It is understood that more than one L- maybe an isostere as long as the substrate analog functions to inhibit aspartic protease function.

Ls which are not isosteres may either be an amide bond or mimetic of an amide bond that is non-hydrolyzable.

X and Y represent molecules which are not typically involved in the recognition by the aspartic protease recognition site, but which do not interfere with recognition. It is preferred that these molecules confer resistance to the degradation of the substrate analog. Preferred examples would be amino acids coupled to the substrate analog through a non-hydrolyzable bond. Other preferred compounds would be capping agents. Still other preferred compounds would be compounds which could be used in the purification of the substrate analogs such as biotin.

As used herein, alkyl refers to substituted or unsubstituted straight, branched or cyclic alkyl groups; and alkoxyl refers to substituted or unsubstituted straight, branched or cyclic alkoxy. Preferably, alkyl and alkoxy groups have from 1 to 40 carbons, and more preferably from 1 to 20 carbons, from 1 to 10 carbons, or from 1 to 3 carbons.

As used herein, alkenyl refers to substituted or unsubstituted straight chain or branched alkenyl groups; alkynyl refers to substituted or unsubstituted straight chain or branched alkynyl groups; alkenyloxy refers to substituted or unsubstituted straight chain or branched alkenyloxy; and alkynyloxy refers to substituted or unsubstituted straight chain or branched alkynyloxy. Preferably, alkenyl, alkynyl, alkenyloxy and alkynyloxy groups have from 2 to 40 carbons, and more preferably from 2 to 20 carbons, from 2 to 10 carbons, or from 2 to 3 carbons.

As used herein, alkaryl refers to an alkyl group that has an aryl substituent; aralkyl refers to an aryl group that has an alkyl substituent; heterocyclic-alkyl refers to a heterocyclic group with an alkyl substituent; alkyl-heterocyclic refers to an alkyl group that has a heterocyclic substituent.

The substituents for alkyl, alkenyl, alkynyl, alkoxy, alkenyloxy, and alkynyloxy groups can be halogen, cyano, amino, thio, carboxy, ester, ether, thioether, carboxamide, hydroxy, or mercapto. Further, the groups can optionally have one or more methylene groups replaced with a heteroatom, such as O, NH or S.

A number of different substrates were tested and analyzed, and the cleavage rules for Memapsin 2 were determined. The results of the substrates which were analyzed are presented in Table 1 and the rules determined from these results are summarized below.

(1) The primary specificity site for a memapsin 2 substrate is subsite position, P_1'. This means that the most important determinant for substrate specificity in memapsin 2 is the amino acid, S1'. P_1' must contain a small side chain for memapsin 2 to recognize the substrate. Preferred embodiments are substrate analogs where R_1 of the P_1' position is either H (side chain of glycine), CH_3 (side chain of alanine), CH_2OH (side chain of serine), or CH_2OOH (side chain of aspartic acid). Embodiments that have an R1 structurally smaller than CH_3 (side chain of alanine) or CH_2OH (side chain of serine) are also preferred.

(2) There are no specific sequence requirements at positions P_4, P_3, P_2, P_1, P_2', P_3', and P_4' Each site can accommodate any other amino acid residue in singularity as long as rule number 3 is met.

(3) At least two of the remaining seven positions, P_4, P_3, P_2, P_1, P_2', P_3', and P_4', must have an R_1 which is made up of a hydrophobic residue. It is preferred that there are at least three hydrophobic residues in the remaining seven positions, P_4, P_3, P_2, P_1, P_2', P_3', and P_4'. Preferred R_1 groups for the positions that contain a hydrophobic group are CH_3 (side chain of alanine), $CH(CH_3)_2$ (side chain of valine), $CH_2CH(CH_3)_2$ (side chain of leucine), $(CH_3)CH(CH_2 CH_3)$ (side chain of isoleucine), CH_2(INDOLE) (side chain of tryptophan), CH_2(Benzene) (side chain of phenylalanine), $CH_2CH_2SCH_3$ (side chain of methionine) CH_2(Phenol) (side chain of tyrosine). It is more preferred that the hydrophobic group be a large hydrophobic group. Preferred R_1s which contain large hydrophobic groups are $CH(CH_3)_2$ (side chain of valine), $CH_2CH(CH_3)_2$ (side chain of leucine), $(CH_3)CH(CH_2 CH_3)$ (side chain of isoleucine), CH_2(Indole) (side chain of tryptophan), CH_2(Benzene) (side chain of phenylalanine), $CH_2CH_2SCH_3$ (side chain of methionine) CH_2(Phenol) (side chain of tyrosine). It is most preferred that positions with a hydrophobic R_1 are $CH(CH_3)_2$ (side chain of valine), $CH_2CH(CH_3)_2$ (side chain of leucine),

CH_2(Benzene) (side chain of phenylalanine), $CH_2CH_2SCH_3$ (side chain of methionine), or CH_2(Phenol) (side chain of tyrosine).

(4) None of the eight positions, P_4, P_3, P_2, P_1, P_1,' P_2', P_3', and P_4' may have a proline side chain at its R1 position.

(5) Not all subsites must have an P represented in the analog. For example, a substrate analog could have X-P_2-L_1-P_1-L_0-P_1'-L_1'-P_2'-L_2'-P_3'-L_3'-Y or it could have X-L_1-P_1-L_0-P_1'-L_1'-P_2'-L_2'-P_3'-L_3'-P_4'L_4'-Y.

Preferred substrate analogs are analogs having the sequences disclosed in Table 1, with the non-hydrolyzable analog between P1 and P1'.

<u>Combinatorial Chemistry to Make Inhibitors</u>

Combinatorial chemistry includes but is not limited to all methods for isolating molecules that are capable of binding either a small molecule or another macromolecule. Proteins, oligonucleotides, and polysaccharides are examples of macromolecules. For example, oligonucleotide molecules with a given function, catalytic or ligand-binding, can be isolated from a complex mixture of random oligonucleotides in what has been referred to as "*in vitro* genetics" (Szostak, <u>TIBS</u> 19:89, 1992). One synthesizes a large pool of molecules bearing random and defined sequences and subjects that complex mixture, for example, approximately 10^{15} individual sequences in 100 µg of a 100 nucleotide RNA, to some selection and enrichment process. Through repeated cycles of affinity chromatography and PCR amplification of the molecules bound to the ligand on the column, Ellington and Szostak (1990) estimated that 1 in 10^{10} RNA molecules folded in such a way as to bind a small molecule dyes. DNA molecules with such ligand-binding behavior have been isolated as well (Ellington and Szostak, 1992; Bock et al, 1992).

Techniques aimed at similar goals exist for small organic molecules, proteins and peptides and other molecules known to those of skill in the art. Screening sets of molecules for a desired activity whether based on libraries of small synthetic molecules, oligonucleotides, proteins or peptides is broadly referred to as combinatorial chemistry.

There are a number of methods for isolating proteins either have *de novo* activity or a modifed activity. For example, phage display libraries have been used for a number of years. A preferred method for isolating proteins that have a given function is described by Roberts and Szostak (Roberts R.W. and Szostak J.W. Proc. Natl. Acad. Sci. USA, 94(23)12997-302 (1997). Another preferred method for combinatorial methods designed to isolate peptides is described in Cohen et al. (Cohen B.A., et al., Proc. Natl. Acad. Sci. USA 95(24):14272-7 (1998)). This method utilizes a modified two-hybrid technology. Yeast two-hybrid systems are useful for the detection and analysis of protein:protein interactions. The two-hybrid system, initially described in the yeast *Saccharomyces cerevisiae*, is a powerful molecular genetic technique for identifying new regulatory molecules, specific to the protein of interest (Fields and Song, *Nature* 340:245-6 (1989)). Cohen et al., modifed this technology so that novel interactions between synthetic or engineered peptide sequences could be identified which bind a molecule of choice. The benefit of this type of technology is that the selection is done in an intracellular environment. The method utilizes a library of peptide molecules that attach to an acidic activation domain. A peptide of choice, for example an extracellular portion of memapsin 2 is attached to a DNA binding domain of a transcriptional activation protein, such as Gal 4. By performing the Two-hybrid technique on this type of system, molecules that bind the extracellular portion of memapsin 2 can be identified.

Screening of Small Molecule Libraries

In addition to these more specialized techniques, methodology well known to those of skill in the art, in combination with various small molecule or combinatorial libraries, can be used to isolate and characterize those molecules which bind to or interact with the desired target, either memapsin 2 or its substrate. The relative binding affinity of these compounds can be compared and optimum inhibitors identified using competitive or non-competitive binding studies which are well known to those of skill in the art. Preferred competitive inhibitors are non-hydrolyzable analogs of memapsin 2. Another will cause

allosteric rearrangements which prevent memapsin 2 from functioning or folding correctly.

Computer assisted Rational Drug Design

Another way to isolate inhibitors is through rational design. This is achieved through structural information and computer modeling. Computer modeling technology allows visualization of the three-dimensional atomic structure of a selected molecule and the rational design of new compounds that will interact with the molecule. The three-dimensional construct typically depends on data from x-ray crystallographic analyses or NMR imaging of the selected molecule. The molecular dynamics require force field data. The computer graphics systems enable prediction of how a new compound will link to the target molecule and allow experimental manipulation of the structures of the compound and target molecule to perfect binding specificity. For example, using NMR spectroscopy, Inouye and coworkers were able to obtain the structural information of N-terminal truncated TSHK (transmembrane sensor histidine kinases) fragments which retain the structure of the individual sub-domains of the catalytic site of a TSHK. On the basis of the NMR study, they were able to identify potential TSHK inhibitors (U.S. Patent No. 6,077,682 to Inouye). Another good example is based on the three-dimensional structure of a calcineurin/FKBP12/FK506 complex determined using high resolution X-ray crystallography to obtain the shape and structure of both the calcineurin active site binding pocket and the auxiliary FKBP12/FK506 binding pocket (U.S. Patent No. 5,978,740 to Armistead). With this information in hand, researchers can have a good understanding of the association of natural ligands or substrates with the binding pockets of their corresponding receptors or enzymes and are thus able to design and make effective inhibitors.

Prediction of molecule-compound interaction when small changes are made in one or both requires molecular mechanics software and computationally intensive computers, usually coupled with user-friendly, menu-driven interfaces between the molecular design program and the user. Examples of molecular modeling systems are the CHARMm and QUANTA programs, Polygen

Corporation, Waltham, MA. CHARMm performs the energy minimization and molecular dynamics functions. QUANTA performs the construction, graphic modeling and analysis of molecular structure. QUANTA allows interactive construction, modification, visualization, and analysis of the behavior of molecules with each other.

A number of articles review computer modeling of drugs interactive with specific proteins, such as Rotivinen, et al., 1988 *Acta Pharmaceutica Fennica* 97, 159-166; Ripka, *New Scientist* 54-57 (June 16, 1988); McKinaly and Rossmann, 1989 *Annu. Rev. Pharmacol. Toxiciol.* 29, 111-122; Perry and Davies, QSAR: Quantitative Structure-Activity Relationships in Drug Design pp. 189-193 (Alan R. Liss, Inc. 1989); Lewis and Dean, 1989 *Proc. R. Soc. Lond.* 236, 125-140 and 141-162; and, with respect to a model enzyme for nucleic acid components, Askew, et al., 1989 *J. Am. Chem. Soc.* 111, 1082-1090. Other computer programs that screen and graphically depict chemicals are available from companies such as BioDesign, Inc., Pasadena, CA., Allelix, Inc, Mississauga, Ontario, Canada, and Hypercube, Inc., Cambridge, Ontario.

Although described above with reference to design and generation of compounds which could alter binding, one could also screen libraries of known compounds, including natural products or synthetic chemicals, and biologically active materials, including proteins, for compounds which alter substrate binding or enzymatic activity.

Screening of Libraries

Design of substrate analogs and rational drug design are based on knowledge of the active site and target, and utilize computer software programs that create detailed structures of the enzyme and its substrate, as well as ways they interact, alone or in the presence of inhibitor. These techniques are significantly enhanced with x-ray crystallographic data in hand. Inhibitors can also be obtained by screening libraries of existing compounds for those which inhibit the catalytically active enzyme. In contrast to reports in the literature relating to memapsin 2, the enzyme described herein has activity analogous to the naturally produced enzyme, providing a means for identifying compounds

which inhibit the endogenous activity. These potential inhibitors are typically identified using high throughput assays, in which enzyme, substrate (preferably a chromogenic substrate) and potential inhibitor (usually screened across a range of concentrations) are mixed and the extent of cleavage of substrate determined. Potentially useful inhibitors are those which decrease the amount of cleavage.

II. Methods of diagnosis and treatment

Inhibitors can be used in the diagnosis and treatment and/or prevention of Alzheimer's disease and conditions associated therewith, such as elevated levels of the forty-two amino acid peptide cleavage product, and the accumulation of the peptide in amyeloid plaques.

Diagnostic Uses

The substrate analogs can be used as reagents for specifically binding to memapsin 2 or memapsin 2 analogs and for aiding in memapsin 2 isolation and purification or characterization, as described in the examples. The inhibitors and purified recombinant enzyme can be used in screens for those individuals more genetically prone to develop Alzheimer's disease.

Therapeutic Uses

Recombinant human memapsin 2 cleaves a substrate with the sequence LVNM/AEGD (SEQ ID NO:9). This sequence is the *in vivo* processing site sequence of human presenilins. Both presenilin 1 and presenilin 2 are integral membrane proteins. They are processed by protease cleavage, which removes the N terminal sequence from the unprocessed form. Once processed, presenilin forms a two-chain heterodimer (Capell et al., J. Biol. Chem. 273, 3205 (1998); Thinakaran et al., Neurobiol. Dis. 4, 438 (1998); Yu et al., Neurosci Lett. 2;254(3):125-8 (1998)), which is stable relative to the unprocessed presenilins. Unprocessed presenilines are quickly degraded (Thinakaran et al., J. Biol. Chem. 272, 28415 (1997); Steiner et al., J. Biol. Chem. 273, 32322 (1998)). It is known that presenilin controls the *in vivo* activity of beta-secretase, which in turn cleaves the amyloid precursor protein (APP) leading to the formation of alpha-beta42. The accumulation of alpha-beta42 in the brain cells is known to be a major cause of Alzheimer's disease (for review, see Selkoe, 1998). The

activity of presenilin therefore enhances the progression of Alzheimer's disease. This is supported by the observation that in the absence of presenilin gene, the production of alpha-beta42 peptide is lowered (De Strooper et al., Nature 391, 387 (1998)). Since unprocessed presenilin is degraded quickly, the processed, heterodimeric presenilin must be responsible for the accumulation of alpha-beta42 leading to Alzheimer's disease. The processing of presenilin by memapsin 2 would enhance the production of alpha-beta42 and therefore, further the progress of Alzheimer's disease. Therefore a memapsin 2 inhibitor that crosses the blood brain barrier can be used to decrease the likelihood of developing or slow the progression of Alzheimer's disease which is mediated by deposition of alpha-beta42. Since memapsin 2 cleaves APP at the beta cleavage site, prevention of APP cleavage at the beta cleavage site will prevent the build up of alpha-beta42.

Vaccines

The catalytically active memapsin 2 or fragments thereof including the active site defined by the presence of two catalytic aspartic residues and substrate binding cleft can be used to induce an immune response to the memapsin 2. The memapsin 2 is administered in an amount effective to elicit blocking antibodies, i.e., antibodies which prevent cleavage of the naturally occurring substrate of memapsin 2 in the brain. An unmodified vaccine may be useful in the prevention and treatment of Alzheimer's disease. The response to the vaccine may be influenced by its composition, such as inclusion of an adjuvant, viral proteins from production of the recombinant enzyme, and/or mode of administration (amount, site of administration, frequency of administration, etc). Since it is clear that the enzyme must be properly folded in order to be active, antibody should be elicited that is active against the endogenous memapsin 2. Antibodies that are effective against the endogenous enzyme are less likely to be produced against the enzyme that is not properly refolded.

Pharmaceutically Acceptable Carriers

The inhibitors will typically be administered orally or by injection. Oral administration is preferred. Alternatively, other formulations can be used for delivery by pulmonary, mucosal or transdermal routes. The inhibitor will usually be administered in combination with a pharmaceutically acceptable carrier. Pharmaceutical carriers are known to those skilled in the art. The appropriate carrier will typically be selected based on the mode of administration. Pharmaceutical compositions may also include one or more active ingredients such as antimicrobial agents, antiinflammatory agents, and analgesics.

Preparations for parenteral administration or administration by injection include sterile aqueous or non-aqueous solutions, suspensions, and emulsions. Examples of non-aqueous solvents are propylene glycol, polyethylene glycol, vegetable oils such as olive oil, and injectable organic esters such as ethyl oleate. Aqueous carriers include water, alcoholic/aqueous solutions, emulsions or suspensions, including saline and buffered media. Preferred parenteral vehicles include sodium chloride solution, Ringer's dextrose, dextrose and sodium chloride, lactated Ringer's, or fixed oils. Intravenous vehicles include fluid and nutrient replenishers, and electrolyte replenishers (such as those based on Ringer's dextrose).

Formulations for topical (including application to a mucosal surface, including the mouth, pulmonary, nasal, vaginal or rectal) administration may include ointments, lotions, creams, gels, drops, suppositories, sprays, liquids and powders. Formulations for these applications are known. For example, a number of pulmonary formulations have been developed, typically using spray drying to formulate a powder having particles with an aerodynanmic diameter of between one and three microns, consisting of drug or drug in combination with polymer and/or surfactant.

Compositions for oral administration include powders or granules, suspensions or solutions in water or non-aqueous media, capsules, sachets, or tablets. Thickeners, flavorings, diluents, emulsifiers, dispersing aids or binders may be desirable.

Peptides as described herein can also be administered as a pharmaceutically acceptable acid- or base- addition salt, formed by reaction with inorganic acids such as hydrochloric acid, hydrobromic acid, perchloric acid, nitric acid, thiocyanic acid, sulfuric acid, and phosphoric acid, and organic acids such as formic acid, acetic acid, propionic acid, glycolic acid, lactic acid, pyruvic acid, oxalic acid, malonic acid, succinic acid, maleic acid, and fumaric acid, or by reaction with an inorganic base such as sodium hydroxide, ammonium hydroxide, potassium hydroxide, and organic bases such as mono-, di-, trialkyl and aryl amines and substituted ethanolamines.

Dosages

Dosing is dependent on severity and responsiveness of the condition to be treated, but will normally be one or more doses per day, with course of treatment lasting from several days to several months or until the attending physician determines no further benefit will be obtained. Persons of ordinary skill can determine optimum dosages, dosing methodologies and repetition rates.

The dosage ranges are those large enough to produce the desired effect in which the symptoms of the memapsin 2 mediated disorder are alleviated (typically characterized by a decrease in size and/or number of amyloid plaque, or by a failure to increase in size or quantity), or in which cleavage of the alpha-beta42 peptide is decreased. The dosage can be adjusted by the individual physician in the event of any counterindications.

The present invention will be further understood by reference to the following non-limiting examples.

Example 1. Cloning of memapsin 2.

1. Cloning and nucleotide sequence of pro-memapsin 2.

New sequences homologous to human aspartic proteases were found in the following entries in the EST IMAGE database: AA136368 pregnant uterus ATCC 947471, AA207232 neurepithelium ATCC 214526, and R55398 human breast ATCC 392689. The corresponding bacterial strains: #947471, #214526, and # 392689 containing the EST sequences were obtained from the ATCC (Rockville, MD). The sequencing of these clones obtained from ATCC

confirmed that they contained sequences not identical to known human aspartic proteases. The completed sequences of these clones assembled into about 80% of prepro-M2 cDNA. Full length cDNAs of these clones were obtained using the following methods.

The Human Pancreas Marathon-Ready cDNA (Clontech), which is double-strand cDNA obtained by reverse-transcription, primer addition, and second strand synthesize of mRNA from human tissues, was used as template for PCR amplification. An adapter primer (AP1) and a nested adapter primer (AP2) were used for 5'- and 3'-RACE PCR. For PCR the 5'-region of the memapsin 2 cDNA, primers AP1 and NHASPR1 were used. Primers for the 3'-end of the cDNA are NHASPF2 and AP1. The middle of the cDNA was amplified by primers NHASPF1 and NHASPR2. The sequence for the primers is as follows: NHASPF1: GGTAAGCATCCCCCATGGCCCCAACGTC (SEQ ID NO:10),
NHASPR1: GACGTTGGGGCCATGGGGGATGCTTACC (SEQ ID NO:11),
NHASPF2: ACGTTGTCTTTGATCGGGCCCGAAAACGAATTGG (SEQ ID NO:12),
NHASPR2: CCAATTCGTTTTCGGGCCCGATCAAAGACAACG (SEQ ID NO:13),
AP1: CCATCCTAATACGACTCACTATAGGGC (SEQ ID NO:14), and
AP2: ACTCACTATAGGGCTCGAGCGGC (SEQ ID NO:15)

Memapsin 2 was also cloned from a human pancreas library (Quick-Screen Human cDNA Library Panel) contained in lambda-gt10 and lambda-gt11 vectors. The primers from the vectors, GT10FWD, GT10REV, GT11FWD, and GT11REV, were used as outside primers. The sequence of the primers used was:
GT10FWD: CTTTTGAGCAAGTTCAGCCTGGTTAA (SEQ ID NO:16),
GT10REV: GAGGTGGCTTATGAGTATTTCTTCCAGGGTA (SEQ ID NO:17),
GT11FWD: TGGCGACGACTCCTGGAGCCCG (SEQ ID NO:18),
GT11REV: TGACACCAGACCAACTGGTAATGG (SEQ ID NO:19).

In addition, memapsin 2 cDNA was amplified directly from the human pancreatic lambda-gt10 and lambda-gt11 libraries. The sequence of the primers was: PASPN1: catatgGCGGGAGTGCTGCCTGCCCAC (SEQ ID NO:20) and

NHASPC1: ggatccTCACTTCAGCAGGGAGATGTCATCAGCAAAGT (SEQ ID NO:21).

The amplified memapsin 2 fragments were cloned into an intermediate PCR vector (Invitrogen) and sequenced.

The assembled cDNA from the fragments, the nucleotide and the deduced protein sequence are shown in SEQ ID NO 1 and SEQ ID NO 2.

Pro-memapsin 2 is homologous to other human aspartic.proteases. Based on the alignments, Pro-memapsin 2 contains a *pro* region, an aspartic protease region, and a trans-membrane region near the C-terminus. The active enzyme is memapsin 2 and its pro-enzyme is pro-memapsin 2.

Example 2. Distribution of memapsin 2 in human tissues.

Multiple tissue cDNA panels from Clontech were used as templates for PCR amplification of a 0.82 kb fragment of memapsin 2 cDNA. The primers used for memapsin 2 were NHASPF1 and NHASPR2. Tissues that contain memapsin 2 or fragments of memapsin 2 yielded amplified PCR products. The amount of amplified product indicated that memapsin 2 is present in the following organs from most abundant to least abundant: pancreas, brain, lung, kidney, liver, placenta, and heart. Memapsin 2 is also present in spleen, prostate, testis, ovary, small intestine, and colon cells.

Example 3. Expression of pro-memapsin 2 cDNA in E. coli, refolding and purification of pro-memapsin 2.

The pro-memapsin 2 was PCR amplified and cloned into the *Bam*HI site of a pET11a vector. The resulting vector expresses pro-memapsin 2 having a sequence from Ala-8p to Ala 326. Figure 1 shows the construction of two expression vectors, pET11-memapsin 2-T1 (hereafter T1) and pET11-memapsin 2-T2 (hereafter T2). In both vectors, the N-terminal 15 residues of the expressed recombinant proteins are derived from the expression vector. Pro-

memapsin 2 residues start at residue Ala-16. The two recombinant pro-memapsin 2s have different C-terminal lengths. Clone T1 ends at Thr- 454 and clone T2 ends at Ala-419. The T1 construct contains a C-terminal extension from the T2 construct but does not express any of the predicted transmembrane domain.

Expression of recombinant proteins and recovery of inclusion bodies

The T1 and T2 expression vectors were separately transfected into *E. coli* strain BL21(DE3). The procedures for the culture of transfected bacteria, induction for synthesis of recombinant proteins and the recovery and washing of inclusion bodies containing recombinant proteins are essentially as previously described (Lin et al., 1994).

Three different refolding methods have produced satisfactory results.

(i) The rapid dilution method.

Pro-memapsin 2 in 8 M urea/100 mM beta-mercaptoethanol with $OD_{280nm} = 5$ was rapidly diluted into 20 volumes of 20 mM-Tris, pH 9.0. The solution was slowly adjusted into pH 8 with 1 M HCl. The refolding solution was then kept at 4° C for 24 to 48 hours before proceeding with purification.

(ii) The reverse dialysis method

An equal volume of 20 mM Tris, 0.5 mM oxidized/1.25 mM reduced glutathione, pH 9.0 is added to rapidly stirred pro-memapsin 2 in 8 M urea/10 mM beta-mercaptoethanol with $OD_{280\ nm} = 5$. The process is repeated three more times with 1 hour intervals. The resulting solution is then dialyzed against sufficient volume of 20 mM Tris base so that the final urea concentration is 0.4 M. The pH of the solution is then slowly adjusted to 8.0 with 1 M HCl.

iii. The preferred method for refolding.

Inclusion bodies are dissolved in 8 M urea, 0.1 M Tris, 1 mM Glycine, 1 mM EDTA, 100 mM beta-mercaptoethanol, pH 10.0. The OD_{280} of the inclusion bodies are adjusted to 5.0 with the 8 M urea solution without beta-mercaptoethanol. The final solution contains the following reducing reagents: 10 mM beta-mercaptoethanol, 10 mM DTT (Dithiothreitol), 1 mM reduced glutathion, and 0.1 M oxidized glutathion. The final pH of the solution is 10.0.

The above solution is rapidly diluted into 20 volumes of 20 mM Tris base, the pH is adjusted to 9.0, and the resulting solution is kept at 4 °C for 16 hr. The solution is equilibrated to room temperature in 6 hr, and the pH is adjusted to 8.5. The solution is returned to 4 °C again for 18 hr.

The solution is again equilibrated to room temperature in 6 hr, and the pH is adjusted to 8.0. The solution is returned to 4 °C again for 4 to 7 days.

The refolding procedures are critical to obtain an enzymically active preparation which can be used for studies of subsite specificity of M2, to analyze inhibition potency of M2 inhibitors, to screen for inhibitors using either random structural libraries or existing collections of compound libraries, to produce crystals for crystallography studies of M2 structures, and to produce monoclonal or polyclonal antibodies of M2.

Purification of recombinant pro-memapsin 2-T2

The refolded material is concentrated by ultrafiltration, and separated on a SEPHACRYL™ S-300 column equilibrated with 20 mM Tris.HCl, 0.4 M urea, pH 8.0. The refolded peak (second peak) from the S-300 column can be further purified with a FPLC RESOURCE-Q™ column, which is equilibrated with 20 mM Tris-HCl, 0.4 M urea, pH 8.0. The enzyme is eluted from the column with a linear gradient of NaCl. The refolded peak from S-300 can also be activated before further purification. For activation, the fractions are mixed with equal volume 0.2 M Sodium Acetate, 70% glycerol, pH 4.0. The mixture is incubated at 22 °C for 18 hr, and then dialyzed twice against 20 volumes of 20 mM Bis-Tris, 0.4 M urea, pH 6.0. The dialyzed materials are then further purified on a FPLC RESOURCE-Q™ column equilibrated with 20 Bis-Tris, 0.4 M urea, pH 6.0. The enzyme is eluted with a linear gradient of NaCl.

SDS-PAGE analysis of the S-300 fractions under reduced and non-reduced conditions indicated that Pro-memapsin 2 first elutes as a very high molecular weight band (greater than about 42 kD) under non-reduced conditions. This indicates that the protein is not folded properly in these fractions, due to disulfide cross linking of proteins. Subsequent fractions contain a protein of predicted pro-memapsin 2-T2 size (about 42 kDa). The pro-

enzyme obtained in these fractions is also proteolytically active for auto-catalyzed activation. These fractions were pooled and subjected to chromatography on the FPLC RESOURCE™ column eluted with a linear gradient of NaCl. Some fractions were analyzed using SDS-PAGE under non-reducing conditions. The analysis showed that fractions 6 and 7 contained most of the active proteins, which was consistent with the first FPLC peak containing the active protein. The main peak was coupled to a shoulder peak, and was present with repeated purification with the same RESOURCE™ Q column. The main shoulder peaks were identified as active pro-memapsin 2 that exist in different conformations under these conditions.

Example 4. Proteolytic activity and cleavage-site preferences of recombinant memapsin 2.

The amino acid sequence around the proteolytic cleavage sites was determined in order to establish the specificity of memapsin 2. Recombinant pro-memapsin 2-T1 was incubated in 0.1 M sodium acetate, pH 4.0, for 16 hours at room temperature in order to create autocatalyzed cleavages. The products were analyzed using SDS-polyacrylamide gel electrophoresis. Several bands which corresponded to molecular weights smaller than that of pro-memapsin 2 were observed. The electrophoretic bands were trans-blotted onto a PVDF membrane. Four bands were chosen and subjected to N-terminal sequence determination in a Protein Sequencer. The N-terminal sequence of these bands established the positions of proteolytic cleavage sites on pro-memapsin 2.

In addition, the oxidized ß-chain of bovine insulin and two different synthetic peptides were used as substrates for memapsin 2 to determine the extent of other hydrolysis sites. These reactions were carried out by auto-activated pro-memapsin 2 in 0.1 M sodium acetate, pH 4.0, which was then incubated with the peptides. The hydrolytic products were subjected to HPLC on a reversed phase C-18 column and the eluent peaks were subjected to electrospray mass spectrometry for the determination of the molecular weight of the fragments. Two hydrolytic sites were identified on oxidized insulin B-chain

(Table1). Three hydrolytic sites were identified from peptide NCH-gamma. A single cleavage site was observed in synthetic peptide PS1-gamma, whose sequence (LVNMAEGD) (SEQ ID NO:9) is derived from the beta-processing site of human presenilin 1 (Table 1).

Table 1: Substrate Specificity of Memapsin 2

Site #	Substrate	P4	P3	P2	P1	P1'	P2'	P3'	P4'	
1	Pro-memapsin 2	R	G	S	M	A	G	V	L	aa 12-18 of SEQ ID No.3
2		G	T	Q	H	G	I	R	L	aa 23-30 of SEQ ID No. 3
3		S	S	N	F	A	V	G	A	aa 98-105 of SEQ ID No. 3
4		G	L	A	Y	A	E	I	A	aa 183-190 of SEQ ID No.3
5	Oxidized insulin B-chain '	H	L	C^	G	S	H	L	V	C^ is cysteic acid; SEQ ID No. 22
6		C^	G	E	R	G	F	F	Y	SEQ ID No. 23
7	Synthetic peptide*				V	G	S	G	V	Three sites cleaved in a peptide: VGSGVLLSRK (SEQ ID NO:30)
8			V	G	S	G	V	L	L	SEQ ID No. 24
9		G	V	L	L	S	R	K		SEQ ID No. 25 SEQ ID No. 26
10	Peptide**	L	V	N	M	A	E	G	D	SEQ ID No. 9

Example 5. Activation of pro-memapsin 2 and enzyme kinetics.

Incubation in 0.1 M sodium acetate, pH 4.0, for 16 h at 22°C auto-catalytically converted *pro*-$M2_{pd}$ to $M2_{pd}$. For initial hydrolysis tests, two synthetic peptides were separately incubated with *pro*-$M2_{pd}$ in 0.1 M Na acetate, pH 4.0 for different periods ranging from 2 to 18 h. The incubated samples

were subjected to LC/MS for the identification of the hydrolytic products. For kinetic studies, the identified HPLC (Beckman System Gold) product peaks were integrated for quantitation. The K_m and k_{cat} values for presenilin 1 and Swedish APP peptides (Table 1) were measured by steady-state kinetics. The individual K_m and k_{cat} values for APP peptide could not be measured accurately by standard methods, so its k_{cat}/K_m value was measured by competitive hydrolysis of mixed substrates against presenilin 1 peptide (Fersht, A. "Enzyme Structure and Mechanism", 2nd Ed., W.H. Freeman and Company, New York. (1985)).

The results are shown in Figures 2A and 2B. The conversion of *pro*-$M2_{pd}$ at pH 4.0 to smaller fragments was shown by SDS-polyacrylamide electrophoresis. The difference in migration between *pro*-$M2_{pd}$ and converted enzyme is evident in a mixture of the two. Figure 2A is a graph of the initial rate of hydrolysis of synthetic peptide swAPP (see Table 1) by $M2_{pd}$ at different pH. Figure 2B is a graph of the relative k_{cat}/K_m values for steady-state kinetic of hydrolysis of peptide substrates by $M2_{pd}$.

Example 6. Expression in Mammalian cells.

Methods

PM2 cDNA was cloned into the *Eco*RV site of vector pSecTag A (Invitrogen). Human APP cDNA was PCR amplified from human placenta 8-gt11 library (Clontech) and cloned into the *Nhe*I and *Xba*I sites of pSecTag A. The procedure for transfection into HeLa cells and vaccinia virus infection for T7-based expression are essentially the same as described by Lin, X., *FASEB J.* 7:1070-1080 (1993).

Transfected cells were metabolically labeled with 200 microCi ^{35}S methionine and cysteine (TransLabel; ICN) in 0.5 ml of serum-free/methionine-free media for 30 min, rinsed with 1 ml media, and replaced with 2 ml DMEM/10% FCS. In order to block vesicle acidification, Bafilomycin A1 was included in the media (Perez, R.G., et al., *J Biol. Chem* 271:9100-9107 (1996)). At different time points (chase), media was removed and the cells were harvested and lysed in 50 mM Tris, 0.3 M NaCl, 5 mM EDTA, 1% Triton X-

100, pH 7.4, containing 10 mM iodoacetamide, 10 :M TPCK, 10 :M TLCK, and 2 microg/ml leupeptin. The supernatant (14,000 x g) of cell lysates and media were immunoadsorbed onto antibody bound to protein G sepharose (Sigma). Anti-APP N-terminal domain antibody (Chemicon) was used to recover the betaN-fragment of APP and anti-alpha-beta $_{1-17}$ antibody (Chemicon, recognizing the N-terminal 17 residues of alpha-beta) was used to recover the 12 kDa ß C-fragment. The former antibody recognized only denatured protein, so media was first incubated in 2 mM dithiothrietol 0.1% SDS at 55°C for 30 min before immunoabsorption. Samples were cooled and diluted with an equal volume of cell lysis buffer before addition of anti-APP N-terminal domain (Chemicon). Beads were washed, eluted with loading buffer, subjected to SDS-PAGE (NOVEX^{TM}) and visualized by autoradiogram or phosphorimaging (Molecular Dynamics) on gels enhanced with Amplify (Amersham). Immunodetection of the betaN-fragment was accomplished by transblotting onto a PVDF membrane and detecting with anti-alpha-beta$_{1-17}$ and chemiluminescent substrate (Amersham).

Results.

HeLa cells transfected with APP or M2 in 4-well chamber slides were fixed with acetone for 10 min and permeabilized in 0.2% Triton X-100 in PBS for 6 min. For localizing M2, polyclonal goat anti-*pro*-M2$_{pd}$ antibodies were purified on DEAE-sepharose 6B and affinity purified against recombinant *pro*-M2$_{pd}$ immobilized on Affigel (BioRad). Purified anti-*pro*-M2$_{pd}$ antibodies were conjugated to Alexa568 (Molecular Probes) according to the manufacturer's protocol. Fixed cells were incubated overnight with a 1:100 dilution of antibody in PBS containing 0.1% BSA and washed 4 times with PBS. For APP, two antibodies were used. Antibody A ß$_{1-17}$ (described above) and antibody Aß$_{17-42}$, which recognizes the first 26 residues following the beta-secretase cleavage site (Chemicon). After 4 PBS washes, the cells were incubated overnight with an anti-mouse FITC conjugate at a dilution of 1:200. Cells were mounted in Prolong anti-fade reagent (Molecular Probes) and visualized on a Leica TCS confocal laser scanning microscope.

Example 7: Design and Synthesis of OM99-1 and OM99-2.

Based on the results of specificity studies of memapsin 2, it was predicted that good residues for positions P1 and P1' would be Leu and Ala. It was subsequently determined from the specificity data that P1' preferred small residues, such as Ala and Ser. However, the crystal structure (determined below in Example 9) indicates that this site can accommodate a lot of larger residues. It was demonstrated that P1' of memapsin 2 is the position with the most stringent specificity requirement where residues of small side chains, such as Ala, Ser, and Asp, are preferred. Ala was selected for P1' mainly because its hydophobicity over Ser and Asp is favored for the penetration of the blood-brain barrier, a requirement for the design of a memapsin 2 inhibitor drug for treating Alzheimer's disease. Therefore, inhibitors were designed to place a transition-state analogue isostere between Leu and Ala (shown as Leu*Ala, where * represents the transition-state isostere, -CH(OH)-CH_2-) and the subsite P4, P3, P2, P2', P3' and P4' are filled with the beta-secretase site sequence of the Swedish mutant from the beta-amyloid protein. The structures of inhibitors OM99-1 and OM99-2 are shown below and in Figures 3A and 3B, respectively:

OM99-1: Val-Asn-Leu*Ala-Ala-Glu-Phe (SEQ. ID NO. 27)
OM99-2: Glu-Val-Asn-Leu*Ala-Ala-Glu-Phe (SEQ. ID NO. 28)

The Leu*Ala dipeptide isostere was synthesized as follows:

The Leu-Ala dipeptide isostere for the M_2-inhibitor was prepared from L-leucine. As shown in Scheme 1, L-leucine was protected as its BOC-derivative 2 by treatment with BOC_2O in the presence of 10% NaOH in diethyl ether for 12 h. Boc-leucine 2 was then converted to Weinreb amide 3 by treatment with isobutyl chcloroformate and N-methylpiperidine followed by treatment of the resulting mixed anhydride with N,O-dimethylhydroxylamine

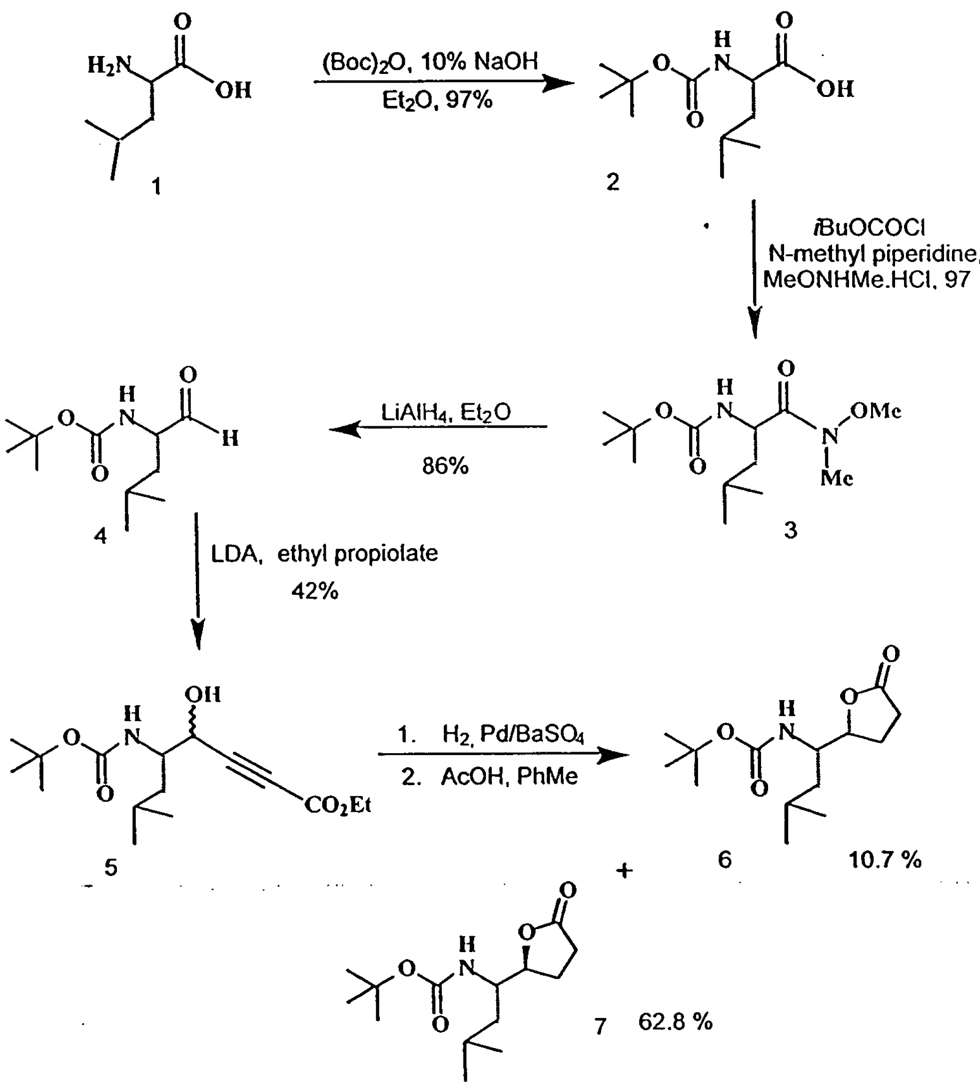

(Scheme 1)

(Nahm and Weinreb, Tetrahedron Letters 1981, 32, 3815). Reduction of 3 with lithium aluminum hydride in diethyl ether provided the aldehyde 4. Reaction of the aldehyde 4 with lithium propiolate derived from the treatment of ethyl

propiolate and lithium diisopropylamide afforded the acetylenic alcohol 5 as an inseparable mixture of diastereomers (5.8:1) in 42% isolated yield (Fray, Kaye and Kleinman, J. Org. Chem. 1986, 51, 4828-33). Catalytic hydrogenation of 5 over Pd/$BaSO_4$ followed by acid-catalyzed lactonization of the resulting gamma-hydroxy ester with a catalytic amount of acetic acid in toluene at reflux, furnished the gamma-lactone 6 and 7 in 73% yield. The isomers were separated by silica gel chromatography by using 40% ethyl acetate in hexane as the eluent.

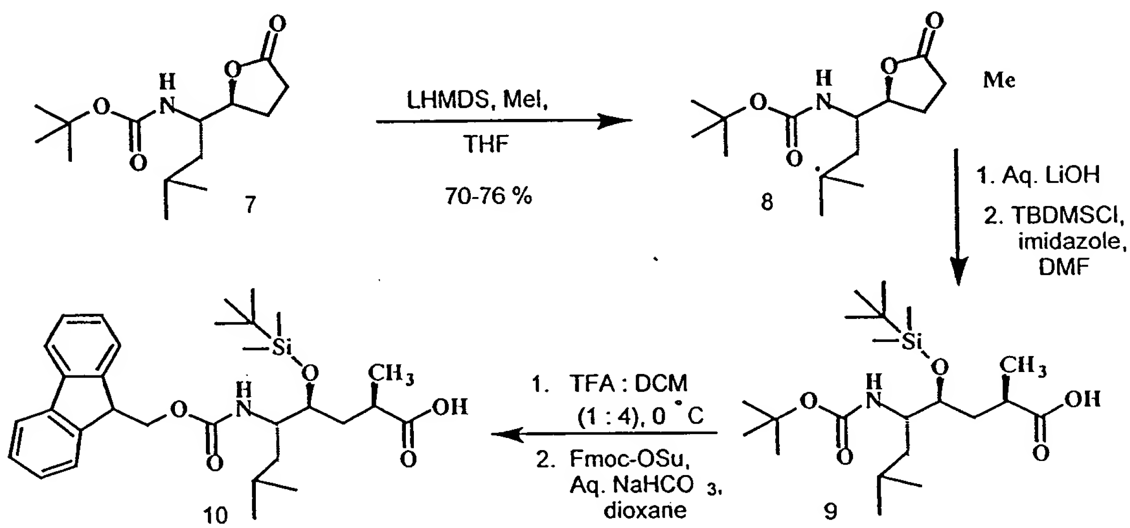

(Scheme 2)

Introduction of the methyl group at C-2 was accomplished by stereoselective alkylation of 7 with methyl iodide (Scheme 2). Thus, generation of the dianion of lactone 7 with lithium hexamethyldisilazide (2.2 equivalents) in tetrahydrofuran at -78°C (30 min) and alkylation with methyl iodide (1.1 equivalents) for 30 min at -78°C, followed by quenching with propionic acid (5 equivalents), provided the desired alkylated lactone 8 (76% yield) along with a small amount (less than 5%) of the corresponding epimer (Ghosh and Fidanze, 1998 J. Org. Chem. 1998, 63, 6146-54). The epimeric cis-lactone was removed by column chromatography over silica gel using a mixture (3:1) of ethyl acetate and hexane as the solvent system. The stereochemical assignment of alkylated lactone 8 was made based on extensive ^{1}H-NMR NOE experiments. Aqueous lithium hydroxide promoted hydrolysis of the lactone 8 followed by protection of the gamma-hydroxyl group with *tert*-butyldimethylsilyl chloride in the

presence of imidazole and dimethylaminopyridine in dimethylformamide afforded the acid 9 in 90% yield after standard work-up and chromatography. Selective removal of the BOC-group was effected by treatment with trifluoroacetic acid in dichloromethane at 0°C for 1 h. The resulting amine salt was then reacted with commercial (Aldrich, Milwaukee) Fmoc-succinimide derivative in dioxane in the presence of aqueous $NaHCO_3$ to provide the Fmoc-protected L*A isostere 10 in 65% yield after chromatography. Protected isostere 10 was utilized in the preparation of a random sequence inhibitor library.

Experimental procedure

N-(tert-Butoxycarbonyl)-L-Leucine (2).

To the suspension of 10 g (76.2 mmol) of L-leucine in 140 mL of diethyl ether was added 80 mL of 10 % NaOH. After all solid dissolves, 20 mL (87.1 mmol) of BOC_2O was added to the reaction mixture. The resulting reaction mixture was stirred at 23°C for 12 h. After this period, the layers were separated and the aqueous layer was acidified to pH 1 by careful addition of 1 N aqueous HCl at 0 °C. The resulting mixture was extracted with ethyl acetate (3 x 100 mL). The organic layers were combined and washed with brine and dried over anhydrous Na_2SO_4. The solvent was removed under reduced pressure to provide title product which was used directly for next reaction without further purification (yield, 97 %). ^1H NMR (400 MHz, $CDCl_3$) δ 4.89 (broad d, 1H, J = 8.3 Hz), 4.31 (m, 1H), 1.74-1.49 (m, 3H), 1.44 (s, 9H), 0.95 (d, 6H, J = 6.5 Hz).

N-(tert-Butoxycarbonyl)-L-leucine-N'-methoxy-N'-methyla-mide (3).

To a stirred solution of N,O-dimethylhydroxyamine hydrochloride (5.52 g, 56.6 mmol) in dry dichloromethane (25 mL) under N_2 atmosphere at 0°C, -methylpiperidine (6.9 mL, 56.6 mmol) was added dropwise. The resulting mixture was stirred at 0°C for 30 min. In a separate flask, N-(tert-butyloxycarbonyl)-L-leucine (1) (11.9 g, 51.4 mmol) was dissolved in a mixture of THF (45 mL) and dichloromethane (180 mL) under N_2 atmosphere. The resulting solution was cooled to –20°C. To this solution was added 1-

methylpiperidine (6.9 mL, 56.6 mmol) followed by isobutyl chloroformate (7.3 mL, 56.6 mmol). The resulting mixture was stirred for 5 minutes at –20°C and the above solution of N,O-dimethylhydroxyamine was added to it. The reaction mixure was kept -20 °C for 30 minutes and then warmed to 23°C. The reaction was quenched with water and the layers were seperated. The aqueous layer was extracted with dichloromethane (3 x 100 mL). The combined organic layers were washed with 10% citric acid, saturated sodium bicarbonate, and brine. The organic layer was dried over anhydrous Na_2SO_4 and concentrated under the reduced pressure. The residue was purified by flash silica gel chromatography (25% ethyl acetate/hexane) to yield the title compound 3 (13.8 g, 97%) as a pale yellow oil. ^{1}H NMR (400 MHz, $CDCl_3$) δ 5.06 (broad d, 1H, J = 9.1 Hz), 4.70 (m, 1H), 3.82 (s, 3H), 3.13 (s, 3H), 1.70 (m, 1H), 1.46-1.36 (m, 2H) 1.41 (s, 9H), 0.93 (dd, 6H, J = 6.5, 14.2 Hz).

N-(tert-Butoxycarbonyl)-L-leucinal (4).

To a stirred suspension of lithium aluminum hydride (770 mg, 20.3 mmol) in dry diethyl ether (60 mL) at -40 °C under N_2 atmosphere, was added N-tert-butyloxycarbonyl-L-leucine-N'-methoxy-N'-methylamide (5.05 g, 18.4 mmol) in diethyl ether (20 mL). The resulting reaction mixture was stirred for 30 min. After this period, the reaction was quenched with 10% $NaHSO_4$ solution (30 mL). The resulting reaction mixture was then warmed to 23°C and stirred at that temperature for 30 min. The resulting solution was filtered and the filter cake was washed by two portions of diethyl ether. The combined organic layers were washed with saturated sodium bicarbonate, brine and dried over anhydrous $MgSO_4$. Evaporation of the solvent under reduced pressure afforded the title aldehyde 4 (3.41 g) as a pale yellow oil. The resulting aldehyde was used immediately without further purification. ^{1}H NMR (400 MHz, $CDCl_3$) δ 9.5 (s, 1H), 4.9 (s, 1H), 4.2 (broad m, 1H), 1.8-1.6 (m, 2H), 1.44 (s, 9H), 1.49-1.39 (m, 1H), 0.96 (dd, 6H, J = 2.7, 6.5 Hz).

Ethyl (4S,5S)-and (4R,5S)-5-[(tert-Butoxycarbonyl)amino]-4-hydroxy-7-methyloct-2-ynoate (5).

To a stirred solution of diisopropylamine (1.1 mL, 7.9 mmol) in dry THF (60 mL) at 0°C under N_2 atmosphere, was added n-BuLi (1.6 M in hexane, 4.95 mL, 7.9 mmol) dropwise. The resulting solution was stirred at 0°C for 5 min and then warmed to 23°C and stirred for 15 min. The mixture was cooled to -78°C and ethyl propiolate (801 µL) in THF (2 mL) was added dropwise over a period of 5 min. The mixture was stirred for 30 min, after which N-Boc-L-leucinal 4 (1.55 g, 7.2 mmol) in 8 mL of dry THF was added. The resulting mixture was stirred at -78°C for 1 h. After this period, the reaction was quenched with acetic acid (5 mL) in THF (20 mL). The reaction mixure was warmed up to 23°C and brine solution was added. The layers were separated and the organic layer was washed with saturated sodium bicarbonate and dried over Na_2SO_4. Evaporation of the solvent under reduced pressure provided a residue which was purified by flash silica gel chromatography (15 % ethyl acetate / hexane) to afford a mixture (3:1) of acetylenic alcohols 5 (0.96 g, 42 %). ^{1}H NMR (300 MHz, $CDCl_3$) δ 4.64 (d, 1H, J = 9.0 Hz), 4.44 (broad s, 1H), 4.18 (m, 2H), 3.76 (m, 1H), 1.63 (m, 1H), 1.43-1.31 (m, 2H), 1.39 (s, 9H), 1.29-1.18 (m, 3H), 0.89 (m, 6H).

(5S,1'S)-5-[1'-[(tert-Butoxycarbonyl)amino]-3'-methylbutyl] -dihydrofuran-2(3H)-one (7).

To a stirred solution of the above mixture of acetylenic alcohols (1.73 g, 5.5 mmol) in ethyl acetate (20 mL) was added 5% Pd/$BaSO_4$ (1 g). The resulting mixture was hydrogenated at 50 psi for 1.5 h. After this period, the catalyst was filtered off through a plug of Celite and the filtrate was concentrated under reduced pressure. The residue was dissolved in toluene (20 mL) and acetic acid (100 µL). The reaction mixure was refluxed for 6 h. After this period, the reaction was cooled to 23°C and the solvent was evaporated to give a residue which was purified by flash silica gel chromatography (40% diethyl ether / hexane) to yield the (5S, 1S')-gamma-lactone 7 (0.94 g, 62.8 and the (5R, 1S')-gamma-lactone 6 (0.16 g, 10.7 %). Lactone 7: ^{1}H NMR (400 MHz, $CDCl_3$) δ 4.50-4.44 (m, 2H), 3.84-3.82 (m, 1H), 2.50 (t, 2H, J = 7.8 Hz), 2.22-2.10 (m, 2H), 1.64-1.31 (m, 3H), 1.41 (s, 9H), 0.91 (dd, 6H, J = 2.2, 6.7

Hz); ^{13}C NMR (75 MHz, $CDCl_3$) δ 177.2, 156.0, 82.5, 79.8, 51.0, 42.2, 28,6, 28.2, 24.7, 24.2, 23.0, 21.9.

(3R,5S,1'S)-5-[1'-[(tert-Butoxycarbonyl)amino)]-3'-methylbut-yl]-3-methyl dihydrofuran-2(3H)-one (8).

To a stirred solution of the lactone 7 (451.8 mg, 1.67 mmol) in dry THF (8 mL) at -78°C under N_2 atmosphere, was added lithium hexamethyldisilazane (3.67 mL, 1.0 M in THF) over a period of 3 min. The resulting mixture was stirred at -78°C for 30 min to generate the lithium enolate. After this period, MeI (228 μL) was added dropwise and the resulting mixture was stirred at –78°C for 20 min. The reaction was quenched with saturated aqueous NH_4Cl solution and was allowed to warm to 23°C. The reaction mixture was concentrated under reduced pressure and the residue was extracted with ethyl acetate (3 x 100 mL). The combined organic layers were washed with brine and dried over anhydrous Na_2SO_4. Evaporation of the solvent afforded a residue which was purified by silica gel chromatography (15 % ethyl acetate / hexane) to furnish the alkylated lactone 8 (0.36 g, 76 %) as an amorphous solid. ^1H NMR (300 MHz, $CDCl_3$) δ 4.43 (broad t, 1H, J = 6.3 Hz), 4.33 (d, 1H, J = 9.6 Hz), 3.78 (m, 1H), 2.62 (m, 1H), 2.35 (m, 1H), 1.86 (m , 1H), 1.63-1.24 (m, 3H), 1.37 (s, 9H), 1.21 (d, 3H, J = 7.5 Hz), 0.87 (dd, 6H, J = 2.6, 6.7 Hz); ^{13}C NMR (75 MHz, $CDCl_3$) δ 180.4, 156.0, 80.3, 79.8, 51.6, 41.9, 34.3, 32.5, 28.3, 24.7, 23.0, 21.8, 16.6.

(2R,4S,5S)-5-[(tert-Butoxycarbonyl)amino]-4-[(tert-butyldimeth -ylsilyl)oxy]-2,7-dimethyloctanoic acid (9).

To a stirred solution of lactone 8 (0.33 g, 1.17 mmol) in THF (2 mL) was added 1 N aqueous LiOH solution (5.8 mL). The resulting mixture was stirred at 23°C for 10 h. After this period, the reaction mixture was concentrated under reduced pressure and the remaining aqueous residue was cooled to 0°C and acidified with 25% citric acid solution to pH 4. The resulting acidic solution was extracted with ethyl acetate (3 x 50 mL). The combined organic layers were washed with brine, dried over Na_2SO_4 and concentrated to yield the

corresponding hydroxy acid (330 mg) as a white foam. This hydroxy acid was used directly for the next reaction without further purification.

To the above hydroxy acid (330 mg, 1.1 mmol) in anhydrous DMF was added imidazole (1.59 g, 23.34 mmol) and tert-butyldimethylchlorosilane (1.76 g, 11.67 mmol). The resulting mixture was stirred at 23°C for 24 h. After this period, MeOH (4 mL) was added and the mixture was stirred for 1 h. The mixure was diluted with 25% citric acid (20 mL) and was extracted with ethyl acetate (3 x 20 mL). The combined extracts were washed with water, brine and dried over anhydrous Na_2SO_4. Evaporation of the solvent gave a viscous oil which was purified by flash chromatography over silica gel (35% ethyl acetate / hexane) to afford the silyl protected acid 9 (0.44 g, 90 %). IR (neat) 3300-3000 (broad), 2955, 2932, 2859, 1711 cm^{-1}; ^1H NMR (400 MHz, DMSO-d^6, 343 K) delta 6.20 (broad s, 1 H), 3.68 (m, 1H), 3.51 (broad s, 1H), 2.49-2.42 (m, 1H), 1.83 (t, 1H, J = 10.1 Hz), 1.56 (m, 1H), 1.37 (s, 9H), 1.28-1.12 (m, 3H), 1.08 (d, 3H, J = 7.1 Hz), 0.87 (d, 3H, J = 6.1 Hz) 0.86 (s, 9 H), 0.82 (d, 3H, J = 6.5 Hz), 0.084 (s, 3H), 0.052 (s, 3H).

(2R,4S,5S)-5-[(fluorenylmethyloxycarbonyl)amino]-4-[(tert-butyldi-methyl silyl)oxy]-2,7-dimethyloctanoic acid (10).

To a stirred solution of the acid 9 (0.17 g , 0.41 mmol) in dichloromethane (2 mL) at 0°C was added trifluoroacetic acid (500 μL). The resulting mixture was stirred at 0°C for 1 h and an additional portion (500 μL) of trifluoroacetic acid was added to the reaction mixture. The mixture was stirred for an additional 30 min and the progress of the reaction was monitored by TLC. After this period, the solvents were carefully removed under reduced pressure at a bath temperature not exceeding 5°C. The residue was dissolved in dioxane (3 mL) and $NaHCO_3$ (300 mg) in 5 mL of H_2O. To this solution was added Fmoc-succinimide (166.5 mg, 0.49 mmol) in 5 mL of dioxane. The resulting mixture was stirred at 23°C for 8 h. The mixure was then diluted with H_2O (5 mL) and acidified with 25% aqueous citric acid to pH 4. The acidic solution was extracted with ethyl acetate (3 x 50 mL). The combined extracts were washed with brine, dried over Na_2SO_4 and concentrated under reduced

pressure to give a viscous oil residue. Purification of the residue by flash chromatography over silica gel afforded the Fmoc-protected acid 10 (137 mg, 61%) as a white foam. ^{1}H NMR (400 MHz, DMSO-d^{6}, 343 K) δ 7.84 (d, 2H, J = 7.4 Hz), 7.66 (d, 2H, J = 8 Hz), 7.39 (t, 2H, J = 7.4 Hz), 7.29 (m, 2H), 6.8 (s, 1H), 4.29-4.19 (m, 3H), 3.74-3.59 (m, 2H), 2.49 (m, 1H), 1.88 (m, 1H), 1.58 (m, 1H), 1.31-1.17 (m, 3H), 1.10 (d, 3H, J = 7.1 Hz), 0.88 (s, 9H), 0.82 (d, 6H, J = 6.2 Hz), 0.089 (s, 3 H), 0.057 (s, 3H).

The synthesis of OM99-1 and OM99-2 were accomplished using solid state peptide synthesis procedure in which Leu*Ala was incorporated in the fourth step. The synthesized inhibitors were purified by reverse phase HPLC and their structure confirmed by mass spectrometry.

Example 8. Inhibition of Memapsin 2 by OM99-1 and OM99-2.

Enzyme activity was measured as described above, but with the addition of either OM99-1 or OM99-2. OM99-1 inhibited recombinant memapsin 2 as shown in FIGURE 4A ~~Figure 5A.~~ The Ki calculated is 3 x 10^{-8} M. The substrate used was a synthetic fluorogenic peptide substrate. The inhibition of OM99-2 on recombinant memapsin 2 was measured using the same fluorogenic substrate. The Ki value was determined to be 9.58 x 10^{-9} M, as shown in FIGURE 4B ~~Figure 5B~~.

These results demonstrate that the predicted subsite specificity is accurate and that inhibitors can be designed based on the predicted specificity.

The residues in P1 and P1' are very important since the M2 inhibitor must penetrate the blood-brain barrier (BBB). The choice of Ala in P1' facilitates the penetration of BBB. Analogues of Ala side chains will also work. For example, in addition to the methyl side chain of Ala, substituted methyl groups and groups about the same size like methyl or ethyl groups can be substituted for the Ala side chain. Leu at P1 can also be substituted by groups of similar sizes or with substitutions on Leu side chain. For penetrating the BBB, it is desirable to make the inhibitors smaller. One can therefore use OM99-1 as a starting point and discard the outside subsites P4, P3, P3' and P4'. The retained structure Asn-Leu*Ala-Ala (SEQ ID NO:29) is then further evolved with substitutions for a tight-binding M2 inhibitor which can also penetrate the BBB.

Example 9. Crystallization and X-ray diffraction study of the protease domain of human memapsin 2 complexed to a specifically designed inhibitor, OM99-2.

The crystallization condition and preliminary x-ray diffraction data on recombinant human memapsin 2 complexed to OM99-2 were determined.

Production of Recombinant Memapsin 2

About 50 mg of recombinant memapsin 2 was purified as described in Example 3. For optimal crystal growth, memapsin 2 must be highly purified. Memapsin 2 was over-expressed from vector pET11a-M2pd. This memapsin 2 is the zymogen domain which includes the pro and catalytic domains to the end of the C-terminal extension but does not include the transmembrane and the intracellular domains. The vector was transfected into E. coli BL21 (DE3) and plated onto ZB agar containing 50 mg/liter ampicillin. A single colony was picked to inoculate 100 ml of liquid ZB containing 5 mg ampicillin and cultured at 30 °C, for 18 hours, with shaking at 220 RPM. Aliquots of approximately 15 ml of the overnight culture were used to inoculate each 1 liter of LB containing 50 mg of ampicillin. Cultures were grown at 37 °C, with shaking at 180 RPM, until an optical density at 600 nm near 0.8 was attained. At that time, expression was induced by addition of 119 mg of IPTG to each liter of culture. Incubation was continued for 3 additional hours post-induction.

Bacteria were harvested, suspended in 50 mM Tris, 150 mM NaCl, pH 7.5 (TN buffer), and lysed by incubation with 6 mg lysozyme for 30 minutes, followed by freezing for 18 hours at -20 °C. Lysate was thawed and made to 1 mM $MgCl_2$ then 1000 Kunitz units of DNAse were added with stirring, and incubated for 30 min. Volume was expanded to 500 ml with TN containing 0.1 % Triton X-100 (TNT buffer) and lysate stirred for 30 minutes. Insoluble inclusion bodies containing greater than 90% memapsin 2 protein were pelleted by centrifugation, and washed by resuspension in TNT with stirring for 1-2 hours. Following three additional TNT washes, the memapsin 2 inclusion bodies were dissolved in 40 ml of 8 M urea, 1 mM EDTA, 1 mM glycine, 100 mM Tris base, 100 mM beta-mercaptoethanlol (8 M urea buffer). Optical

density at 280 nm was measured, and volume expanded with 8 M urea buffer to achieve final O.D. near 0.5, with addition of sufficient quantity of beta-mercaptoethanol to attain 10 mM total, and 10 mM DTT, 1 mM reduced glutathione, 0.1 mM oxidized glutathione. The pH of the solution was adjusted to 10.0 or greater, and divided into four aliquots of 200 ml each. Each 200 ml was rapidly-diluted into 4 liters of 20 mM Tris base, with rapid stirring. The pH was adjusted immediately to 9.0, with 1 M HCl, and stored at 4 °C overnight. The following morning the diluted memapsin 2 solution was maintained at room temperature for 4-6 hours followed by adjusting pH to 8.5 and replacing the flasks to the 4 °C room. The same procedure was followed the next day with adjustment of pH to 8.0.

This memapsin 2 solution was allowed to stand at 4 °C for 2-3 weeks. The total volume of approximately 16 liters was concentrated to 40 mls using ultra-filtration (Millipore) and stir-cells (Amicon), and centrifuged at 140,000 xg at 30 minutes in a rotor pre-equilbrated to 4 °C. The recovered supernatant was applied to a 2.5 x 100 cm column of S-300 equilibrated in 0.4 M urea, 20 mM Tris-HCl, pH 8.0, and eluted with the same buffer at 30 ml/hour. The active fraction of memapsin 2 was pooled and further purified in a FPLC using a 1 ml Resource-Q (Pharmacia) column. Sample was filtered, and applied to the Resource-Q column equilibrated in 0.4 M urea, 50 mM Tris-HCl, pH 8.0. Sample was eluted with a gradient of 0 - 1 M NaCl in the same buffer, over 30 ml at 2 ml/min. The eluents containing memapsin 2 appeared near 0.4 M NaCl which was pooled for crystallization procedure at a concentration near 5 mg/ml.

The amino-terminal sequence of the protein before crystallization showed two sequences starting respectively at residues 28p and 30p. Apparently, the pro peptide of recombinant pro-memapsin 2 had been cleaved during the preparation by a yet unidentified proteolytic activity.

The activation of the folded pro-enzyme to mature enzyme, memapsin 2, was carried out as described above, i.e., incubation in 0.1 M sodium acetate pH 4.0 for 16 hours at 22 °C. Activated enzyme was further purified using anion-exchange column chromatography on Resource-Q anion exchange column. The

purity of the enzyme was demonstrated by SDS-gel electrophoresis. At each step of the purification, the specific activity of the enzyme was assayed as described above to ensure the activity of the enzyme.

Preliminary Crystallization with OM99-2

Crystal trials were performed on purified memapsin 2 in complex with a substrate based transition-state inhibitor OM99-2 with a Ki = 10 nM. OM99-2 is equivalent to eight amino-acid residues (including subsites S4, S3, S2, S1 S1', S2', S3' and S4' in a sequence EVNLAAEF) with the substitution of the peptide bond between the S1 and S1' (L-A) by a transition-state isostere hydroxyethylene. Purified M2 was concentrated and mixed with 10 fold excessive molar amount of inhibitor. The mixture was incubated at room temperature for 2-3 hours to optimize the inhibitor binding. The crystallization trial was conducted at 20 °C using the hanging drop vapor diffusion procedure. A systemic search with various crystallization conditions was conducted to find the optimum crystallization conditions for memapsin 2/OM99-2 inhibitor complex. For the first step, a coarse screen aimed at covering a wide range of potential conditions were carried out using the Sparse Matrix Crystallization Screen Kits purchased from Hampton Research. Protein concentration and temperature were used as additional variables. Conditions giving promising (micro) crystals were subsequently used as starting points for optimization, using fine grids of pH, precipitants concentration etc.

Crystals of memapsin-inhibitor complex were obtained at 30% PEG 8000, 0.1 M NaCocadylate, pH 6.4. SDS gel electrophoresis of a dissolved crystal verified that the content of the crystal to be memapsin 2. Several single crystals (with the sizes about 0.3 mm x 0.2 mm x 0.1 mm) were carefully removed from the cluster for data collection on a Raxis IV image plate. These results showed that the crystals diffract to 2.6 Å. ~~A typical protein diffraction pattern is shown in Figure 6.~~ An X-ray image visualization and integration software–Denzo, was used to visualize and index the diffraction data. Denzo identified that the primitive orthorhombic lattice has the highest symmetry with a significantly low distortion index. The unit cell parameters were determined

as: a=89.1 Å, b=96.6 Å, c=134.1 Å, $\alpha=\beta=\gamma=90^o$. There are two memapsin 2/OM99-2 complexes per crystallographic asymmetric unit, the V_m of the crystal is 2.9 $Å^3$/Da. Diffraction extinctions suggested that the space group is $P2_12_12_1$.

With diffraction of the current crystal to 2.6 Å, the crystal structure obtained from these data has the potential to reach atomic solution, i.e., the three-dimensional positions of atoms and chemical bonds in the inhibitor and in memapsin 2 can be deduced. Since memapsin 2 sequence is homologous with other mammalian aspartic proteases, e.g., pepsin or cathepsin D, it is predicted that the three dimensional structures of memapsin 2 will be similar (but not identical) to their structures. Therefore, in the determination of x-ray structure from the diffraction data obtained from the current crystal, it is likely the solution of the phase can be obtained from the molecular replacement method using the known crystal structure of aspartic proteases as the search model.

Further Crystallization Studies

Concentrated memapsin 2 was mixed with 10-fold molar excessive of the inhibitor. The mixture was incubated at room temperature for 2-3 hours to optimize inhibitor binding, and then clarified with a 0.2 micron filter using centrifugation. Crystals of memapsin 2-inhibitor complex were grown at 20 °C by hanging drop vapor diffusion method using equal volumes of enzyme-inhibitor and well solution. Crystals of quality suitable for diffraction studies were obtained in two weeks in 0.1 M sodium cacodylate, pH 7.4, 0.2 M $(NH_4)_2SO_4$, and 22.5% PEG8000. The typical size of the crystals was about 0.4 x 0.4 x 0.2 mm^3.

Diffraction data were measured on a Raxis-IV image plate with a Rigaku X-ray generator, processed with the HKL program package [Z. Otwinowski, W. Minor, Methods Enzymol. 276, 307 (1997)] A single crystal of approximately 0.4 x 0.4 x 0.2 mm^3 in size was treated with a cryo-protection solution of 25% PEG8000, 20% glycerol, 0.1 M sodium-cacodylate pH 6.6, and 0.2 M $(NH_4)_2SO_4$, and then flash-cooled with liquid nitrogen to about –180 °C for data collection. Diffraction was observed to at least 1.9 Å. The crystal form

belongs to space group $P2_1$ with two memapsin 2/OM99-2 complexes per crystallographic asymmetric unit and 56% solvent content.

Molecular replacement was performed with data in the range of 15.0-3.5 Å using program AmoRe, CCP4 package [Navaza, J., Acta Crystallog. Sect. A. 50, 157 (1994)]. Pepsin, a human aspartic protease with 22% sequence identity, was used as the search model(PDB id 1psn). Rotation and translation search, followed by rigid body refinement, identified a top solution and positioned both molecules in the asymmetric unit. The initial solution had a correlation coefficient of 22% and an R-factor of 0.51. The refinement was carried out using the program CNS [Brunger et al., Acta Crystallogr. Sect. D, 54, 905 (1998)]. 10% of reflections were randomly selected prior to refinement for R_{free} monitoring [Bruger, A.T., X-PLOR Version 3.1: A system for X-ray Crystallography and NMR, Yale University Press, New Haven, CT (1992)]. Molecular graphics program [Jones, T.A., et al., Improved methods for building protein models in electron denisty maps and location of errors in these models. Acta Crystallogr. Sect. A 47, 110 (1991)] was used for map display and model building. From the initial pepsin model, corresponding amino acid residues were changed to that of memapsin 2 according to sequence alignment. The side chain conformations were decided by the initial electron density map and a rotomer library. This model was refined using molecular dynamics and energy minimization function of CNS [Bruger, A.T., et al., Acta Crystallogr. Sect. D, 54, 905 (1998)]. The first cycle of refinement dropped the $R_{working}$ to 41% and the R_{free} to 45%. At this stage, electron densities in the omit map clearly showed the inhibitor configuration in the active site cleft. Structural features unique to memapsin 2 in chain tracing, secondary structure, insertions, deletions and extensions (as compared to the search model) are identified and constructed in subsequent iterations of crystallographic refinement and map fitting. The inhibitor was built into the corresponding electron density.

About 440 solvent molecules were then gradually added to the structure as identified in the |Fo|-|Fc| map contoured at the 3 sigma level. Non-crystallographic symmetry restriction and averaging were used in early stages

of refinement and model building. Bulk solvent and anisotropic over-all B factor corrections were applied through the refinement. The final structure was validated by the program PROCHECK Laskowski, R.A. et al., J. Appl. Crystallog. 26, 283 (1993) which showed that 95% of the residues are located in the most favored region of the Ramachandran plot. All the main chain and side chain parameters are within or better than the standard criteria. The final $R_{working}$ and R_{free} are 18% and 22% respectively. Refinement statistics are listed in Table 2.

Table 2. Data Collection and Refinement Statistics

A. Data Statistics	
Space group	$P2_1$
Unit Cell (a, b, and c in Å)	53.7, 85.9, 109.2
(, , and in degrees)	90.0, 101.4, 90.0
Resolution ( )	25.0-1.9
Number of observed reflections	144,164
Number of unique reflections	69,056
R_{merge} [a]	0.061 (0.25)
Data completeness (%) (25.0-1.9)	90.0 (68.5)
<I/ (I)>	13.7 (3.0)
B. Refinement Statistics	
$R_{working}$ [b]	0.186
R_{free} [b]	0.228
RMS deviation from ideal values	
Bond length (Å)	0.014
Bond angle (Deg)	1.7
Number of water molecules	445
Average B-factor (^{2})	
Protein	28.5
Solvent	32.2

[a] $R_{merge} = \ _{hkl}\ _{i} | I_{hkl,i} - \langle I_{hkl} \rangle | / \ _{hkl} \langle I_{hkl} \rangle$, where $I_{hkl,i}$ is the intensity of the ith measurement and $\langle I_{hkl} \rangle$ is the weighted mean of all measurements of I_{hkl}.
[b] $R_{working\ (free)} = \ | F_o| - | F_c| / \ | F_o|$, where F_o and F_c are the observed and calculated structure factors. Numbers in parentheses are the corresponding numbers for the highest resolution shell (2.00-1.9 Å). Reflections with $F_o/\ (F_o)$>=0.0 are included in the refinement and R factor calculation.

Memapsin 2 Crystal Structure.

The bilobal structure of memapsin 2 (Figure 7) is characteristic of aspartic proteases (Tang, J., et al., Nature 271, 618-621 (1978)) with the conserved folding of the globular core. The substrate binding cleft, where the inhibitor is bound ~~(Figure 7)~~ FIGURE 6, is located between the two lobes. A pseudo two-fold symmetry between the N- (residues 1-180) and C- (residues 181-385) lobes ~~(Figure 7)~~ FIGURE 6, which share 61 superimposable atoms with an overall 2.3 Å rms deviation using a 4 Å cutoff. The corresponding numbers for pepsin are 67 atoms and 2.2 Å. Active-site Asp[32] and Asp[228] and the surrounding hydrogen-bond network are located in the center of the cleft ~~(Figure 7)~~ FIGURE 6 and are conserved with the typical active-site conformation (Davies, D. R., Annu. Rev. Biophys. Chem. 19, 189 (1990)). The active site carboxyls are, however, not co-planar and the degree of which (50°) exceeds those observed previously.

Compared to pepsin, the conformation of the N-lobe is essentially conserved (Sielecki et al., 1990). The most significant structural differences are the insertions and a C-terminal extension in the C-lobe. Four insertions in helices and loops ~~(Figure 7)~~ FIGURE 6 are located on the adjacent molecular surface. Insertion F, which contains four acidic residues, is the most negatively charged surface on the molecule. Together, these insertions enlarged significantly the molecular boundary of memapsin 2 as compared to pepsin ~~(Figure 8).~~ FIGURE 7 These surface structural changes may have function in the association of memapsin 2 with other cell surface components. Insertions B and E are located on the other side of the molecule ~~(Figure 7).~~ FIGURE 6 The latter contains a beta-strand that paired with part of the C-terminal extension G. A six- residue deletion occurs at position 329 on a loop facing the flap on the opposite side of the active-site cleft, resulting in an apparently more accessible cleft. Most of the C-terminal extension (residues 359-393) is in highly ordered structure. Residues 369-376 form a beta structure with 7 hydrogen bonds to strand 293-299, while residues 378-383 form a helix ~~(Figures 7 and 8).~~ FIGURES 6 AND 7 Two disulfide pairs (residues 155/359 and 217/382) unique to memapsin 2 fasten both ends of the extension region to the C-lobe. This C-terminal extension is much longer than those observed

previously and is conformationally different [Cutfield, S. M., et al., Structure 3, 1261 (1995); Abad-Zapatero, C., et al., Protein Sci. 5, 640 (1996); Symersky, J. et al., Biochemistry 36, 12700 (1997); Yang, J., et al., Acta Crystallogr. D 55, 625 (1999)]. The last eight residues (386-393) are not seen in the electron density map; they may form a connecting stem between the globular catalytic domain and the membrane anchoring domain.

Of the 21 putative pro residues only the last six, 43p-48p, are visible in the electron density map. The remainders are likely mobile. Pro-memapsin expressed in mammalian cell culture has an N-terminus position at Glu^{33p}. However, an Arg-Arg sequence present at residues 43p-44p is a frequent signal for pro-protein processing, e.g., in prorenin (Corvol, P. et al., Hypertension 5, 13-9 (1983)). Recombinant memapsin 2 derived from this cleavage is fully active. The mobility of residues 28p-42p suggests that they are not part of the structure of mature memapsin 2.

<u>Memapsin 2-OM99-2 Interaction.</u>

The binding of the eight-residue inhibitor OM99-2 in the active-site cleft shares some structural features with other aspartic protease-inhibitor complexes [Davies, D.R., Annu. Rev. Biophys. Chem. 19, 189 (1990); Bailey and Cooper, (1994); Dealwis et al., (1994)]. These include four hydrogen bonds between the two active-site aspartics to the hydroxyl of the transition-state isostere, the covering of the flap (residues 69-75) over the central part of the inhibitor and ten hydrogen bonds to inhibitor backbone ~~(Figure 9).~~ Figures 8+9 Most of the latter are highly conserved among aspartic proteases [Davies, D. R. Annu. Rev. Biophys. Chem. 19, 189 (1990); Bailey and Cooper, (1994); Dealwis et al., (1994)] except that hydrogen bonds to Gly^{11} and Tyr^{198} are unique to memapsin 2. These observations illustrate that the manner by which memapsin 2 transition-state template for substrate peptide backbone and mechanism of catalysis are similar to other aspartic proteases. These common features are, however, not the decisive factors in the design of specific memapsin 2 inhibitors with high selectivity.

The observation important for the design of inhibitor drugs is that the memapsin 2 residues in contact with individual inhibitor side chains ~~(Figure 9)~~ FIGURE 8 are quite different from those for other aspartic proteases. These side chain contacts are important for the design of tight binding inhibitor with high selectivity. Five N-terminal residues of OM99-2 are in extended conformation and, with the exception of P_1' Ala, all have clearly defined contacts (within 4 Å of an inhibitor side chain) with enzyme residues in the active-site cleft (Figure 8 ~~9~~).

The protease S_4 subsite is mostly hydrophilic and open to solvent. The position of inhibitor P_4 Glu side chain is defined by hydrogen bonds to Gly^{11} and to P_2 Asn ~~(Figure 9)~~ FIGURE 8 and the nearby sidechains of Arg^{235} and Arg^{307}, which explains why the absence of this residue from OM99-2 cause a 10-fold increase in K_i. Likewise, the protease S_2 subsite is relatively hydrophilic and open to solvent. Inhibitor P_2 Asn side chain has hydrogen bonds to P_4 Glu and Arg^{235}. The relatively small S_2 residues Ser^{325} and Ser^{327} (Gln and Met respectively in pepsin) may fit a side chain larger than Asn. Memapsin 2 S_1 and S_3 subsites, which consist mostly of hydrophobic residues, have conformations very different from pepsin due to the deletion of pepsin helix h_{H2} (Dealwis, et al., (1994)). The inhibitor side chains of P_3 Val and P_1 Leu are closely packed against each other and have substantial hydrophobic contacts with the enzyme ~~(Figure 9),~~ FIGURE 8 especially P_3 interacts with Tyr^{71} and Phe^{108}. In the beta- secretase site of native APP, the P_2 and P_1 residues are Lys and Met respectively. Swedish mutant APP has Asn and Leu in these positions respectively, resulting in a 60-fold increase of k_{cat}/K_m over that for native APP and an early onset of AD described by Mullan, M., et al. [Nat. Genet. 2, 340 (1992)]. The current structure suggests that inhibitor P_2 Lys would place its positively charge in an unfavorable interaction with Arg^{235} with a loss of hydrogen bond to Arg^{235}, while P_1 Met would have less favorable contact with memapsin 2 than does leucine in this site ~~(Figure 10). N~~ FIGURE 9 o close contact with memapsin 2 was seen for P_1' Ala and an aspartic at this position, as in APP, may be accommodated by interacting with Arg^{228}.

The direction of inhibitor chain turns at P_2' and leads P_3' and P_4' toward the protein surface FIGURE 9 ~~(Figure 10).~~ As a result, the side-chain position of P_2' Ala deviates from the regular extended conformation. The side chains of P_3' Glu and P_4' Phe are both pointed toward molecular surface with little significant interaction with the protease (Figure 10). The relatively high B-factors (58.2 $Å^2$ for Glu and 75.6 $Å^2$ for Phe) and less well-defined electron density suggests that these two residues are relatively mobile, in contrast to the defined structure of the S_3' and S_4' subsites in renin-inhibitor (CH-66) complex (Dealwis et al., 1994). The topologically equivalent region of these renin subsites (residues 292 - 297 in pepsin numbering) is deleted in memapsin 2. These observations suggest that the conformation of three C-terminal residues of OM99-2 may be a functional feature of memapsin 2, possibly a way to lead a long protein substrate out of the active-site cleft.

Example 10: Using The Crystal Structure to Design Inhibitors.

Pharmaceutically acceptable inhibitor drugs normally post a size limit under 800 daltons. In the case of memapsin 2 inhibitors, this requirement may even be more stringent due to the need for the drugs to penetrate the blood-brain barrier [Kearney and Aweeka, (1999)]. In the current model, well defined subsite structures spending P_4 to P_2' provide sufficient template areas for rational design of such drugs. The spacial relationships of individual inhibitor side chain with the corresponding subsite of the enzyme as revealed in this crystal structure permits the design of new inhibitor structures in each of these positions. It is also possible to incorporate the unique conformation of subsites P_2', P_3' and P_4' into the selectivity of memapsin 2 inhibitors. The examples of inhibitor design based on the current crystal structure are given below.

Example A: Since the side chains of P_3 Val and P_1 Leu are packed against each other and there is no enzyme structure between them, cross-linking these side chains would increase the binding strength of inhibitor to memaspin 2. This is because when binding to the enzyme, the cross-linked inhibitors would have less entropy difference between the free and bound forms than their non-cross-linked counterparts [Khan, A.R., et al., Biochemistry, 37, 16839

(1998)]. Possible structures of the cross-linked side chains include those shown in ~~Figure 11.~~ Figure 10

Example B: The same situation exits between the P4 Glu and P2 Asn. The current crystal structure shows that these side chains are already hydrogen bonded to each other so the cross linking between them would also derive binding benefit as described in the Example A. The cross-linked structures include those shown in ~~Figure 12.~~ Figure 11

Example C: Based on the current crystal structure, the P1' Ala side chain may be extended to add new hydrophobic, Van der Waals and H-bond interactions. An example of such a design is diagramed in ~~Figure 13.~~ Figure 12

Example D: Based on the current crystal structure, the polypeptide backbone in the region of P1, P2, and P3, and the side chain of P1-Leu can be bridged into rings by the addition of two atoms (A and B in ~~Figure 14).~~ Figure 12 Also, a methyl group can be added to the beta-carbon of the P1-Leu ~~(Figure 14).~~ Figure 13

Modifications and variations of the methods and materials described herein will be obvious to those skilled in the art and are intended to come within the scope of the appended claims.